INTERNATIONAL JOURNAL OF
Minerals, Metallurgy and Materials

Volume 31, Number 6, June 2024
Page 1263

Invited Review

https://doi.org/10.1007/s12613-023-2754-y

Development in oxide metallurgy for improving the weldability of high-strength low-alloy steel—Combined deoxidizers and microalloying elements

Tingting Li and Jian Yang✉

State Key Laboratory of Advanced Special Steel, School of Materials Science and Engineering, Shanghai University, Shanghai 200444, China
(Received: 13 June 2023; revised: 10 September 2023; accepted: 26 September 2023)

Abstract: The mechanisms of oxide metallurgy include inducing the formation of intragranular acicular ferrite (IAF) using micron-sized inclusions and restricting the growth of prior austenite grains (PAGs) by nanosized particles during welding. The chaotically oriented IAF and refined PAGs inhibit crack initiation and propagation in the steel, resulting in high impact toughness. This work summarizes the combined effect of deoxidizers and alloying elements, with the aim to provide a new perspective for the research and practice related to improving the impact toughness of the heat affected zone (HAZ) during the high heat input welding. Ti complex deoxidation with other strong deoxidants, such as Mg, Ca, Zr, and rare earth metals (REMs), can improve the toughness of the heat-affected zone (HAZ) by refining PAGs or increasing IAF contents. However, it is difficult to identify the specific phase responsible for IAF nucleation because effective inclusions formed by complex deoxidation are usually multiphase. Increasing alloying elements, such as C, Si, Al, Nb, or Cr, contents can impair HAZ toughness. A high C content typically increases the number of coarse carbides and decreases the potency of IAF formation. Si, Cr, or Al addition leads to the formation of undesirable microstructures. Nb reduces the high-temperature stability of the precipitates. Mo, V, and B can enhance HAZ toughness. Mo-containing precipitates present good thermal stability. VN or V(C,N) is effective in promoting IAF nucleation due to its good coherent crystallographic relationship with ferrite. The formation of the B-depleted zone around the inclusion promotes IAF formation. The interactions between alloying elements are complex, and the effect of adding different alloying elements remains to be evaluated. In the future, the interactions between various alloying elements and their effects on oxide metallurgy, as well as the calculation of the nucleation effects of effective inclusions using first principles calculations will become the focus of oxide metallurgy.

Keywords: oxide metallurgy technology; heat affected zone; high-strength low-alloy steel; intragranular acicular ferrite; microalloying element

1. Introduction

High-strength low-alloy (HSLA) steels with microalloying were developed from low-carbon (C) steels in the 1950s and have been widely utilized as structural materials [1–2]. These steels contain small amounts of alloying elements, such as Ti, Nb, V, which can enhance the strength through solid solution strengthening and precipitation strengthening, such as the formation of stable carbides, nitrides, or carbonitrides. Nowadays, the application of HSLA steels has been expanded to almost all fields, such as construction [3], machinery [4], shipbuilding [5], ocean engineering equipment [6–8], bridges [9], oil and gas pipelines [10], and other fields [11–12].

Welding is the most frequently used connection method in the fabrication of HSLA steels. With the development of welding technologies, the welding heat input continuously increases, having exceeded 50 kJ·cm^{-1}; in some cases of high heat input welding (HHIW), the heat input even reaches up to 100 kJ·cm^{-1} or higher, which can lead to enhanced welding efficiency and reduced welding cost [13–15]. Adding C and other alloying elements into steels to obtain a high strength leads to increased carbon equivalent (C_{eq}) and decreased toughness of the heat-affected zone (HAZ) [16]. Despite the rapid development of thermomechanically controlled processing (TMCP) [17], which can enhance the steel strength with a relatively low C_{eq} and thereby improve HAZ toughness, achieving an excellent HAZ toughness after welding with the high heat input greater than 300 kJ·cm^{-1} remains challenging [18–19]. HHIW usually involves a long residence time at high temperatures and a low cooling rate, which inevitably leads to the remarkably coarsening of prior austenite grains (PAGs) and the formation of brittle microstructures that result in reduced HAZ toughness. The deterioration of the microstructures and toughness of HAZ seriously affects the production and service safety of the large equipment and structure. For the service safety of steel structures, maintaining the superior performance of HAZ (specifically its low-temperature toughness) has become a research hotspot in the application of HHIW [11,20–22].

In the past few decades, oxide metallurgy has become an

✉ Corresponding author: Jian Yang E-mail: yang_jian@t.shu.edu.cn

important technology to improve the low-temperature impact toughness of HAZ. The collaborative efforts of numerous researchers have resulted in the success of this technology. Several studies have reviewed the progress in oxide metallurgy technology from different aspects. Mu *et al.* [23], Sarma *et al.* [24], Babu [25], and Koseki [26] provided comprehensive reviews on the relationship between inclusions and microstructures and revealed the transformation mechanism of microstructures. Shao *et al.* [27] focused on the formation mechanisms of intragranular acicular ferrite (IAF) and reviewed the effects of austenitizing conditions, continuous cooling rate, and isothermal quenching time and temperature on IAF transformation. Ma *et al.* [28] explored the effective inclusions that can act as the nucleation sites for IAF. Liang *et al.* [29] and Pan *et al.* [30] summarized the background of oxide metallurgy technology and focused on the application of rare earth metals (REMs) in improving the HAZ microstructures.

In recent years, extensive investigations have been conducted on the formation of oxides of Ti, Zr, Ca, and Mg in steels to improve the weldability of HSLA steels, especially after HHIW. However, previous reviews mainly focused on the formation mechanism and influence factors of IAF transformation. The effects of deoxidation methods, especially alloying elements, on IAF nucleation and HAZ microstructures under oxide metallurgy conditions have not been summarized. Therefore, the current overview clarifies the influences of deoxidizers, such as Ti, Mg, Ca, Zr, and REMs, and microalloying elements, such as C, Si, Al, Nb, V, Cr, Mo, and B, on IAF nucleation and HAZ microstructures after HHIW based on recent studies. The development of oxide metallurgy in practice is also evaluated.

2. Fundament and industrial application of oxide metallurgy technology

2.1. Fundament of oxide metallurgy technology

2.1.1. Characteristics and microstructures of HAZ

The microstructure and temperature range of HAZ in HSLA steel subjected to HHIW are shown in Fig. 1 [31]. The HAZ usually includes five parts: fusion zone (>1500°C), coarse-grained zone (1100–1500°C), fine-grained zone (1100°C–A_{c3}), two phase zone (A_{c3}–A_{c1}), and temper zone (<A_{c1}). Brittle microstructures, such as ferrite side plate (FSP), grain boundary ferrite (GBF), and upper bainite (UB), are easily generated in the coarse-grained heat affected zone (CGHAZ), resulting in a decline in strength and toughness after the welding thermal cycle. Therefore, the CGHAZ near the welded fusion line is generally known as the local brittle zone in the HAZ.

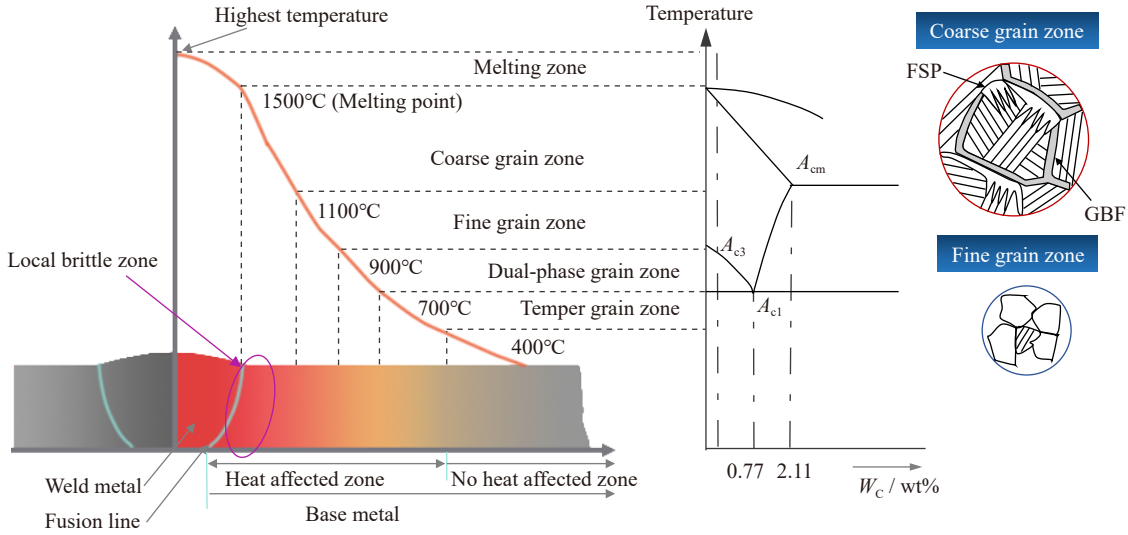

Fig. 1. Schematic of temperature distribution and microstructures near the fusion line during high heat input welding. A_{c3}—the start temperature for the transformation from pearlite into austenite; A_{c1}—the finish temperature for the transformation from ferrite to austenite; A_{cm}—the boundary temperature between the γ austenite and the austenite/cementite field; W_C—carbon content. Reprinted from Ref. [31].

During the austenite–ferrite transformation in welding, two or more various microstructural constituents are formed in each austenite grain. The HAZ microstructures depend on the steel compositions, thermal history during welding, and other factors [29]. For HSLA steels with low C_{eq}, the HAZ microstructures are mainly ferrite. The microstructures of ferrite are usually classified according to their shapes, including IAF, GBF, FSP, and others. By comparison, alloy steels with high C_{eq} have higher strength grades and better quenching permeability than those with low C_{eq}. Under HHIW, the development of IAF becomes challenging and is replaced by low-temperature-transformation microstructures, such as upper bainite (UB) and martensite, due to the decrease in transformation temperature [32]. This phenomenon has a detrimental effect on HAZ toughness because UB, martensite, and martensite–austenite (M–A) constituents or carbides are likely to provide preferential sites for crack nucleation and propagation paths [26,33].

GBFs and FSPs are easily nucleated at grain boundaries, and FSPs usually have sheet structures parallel to the crystal

orientation [34]. IAF is the optimal microstructure combining excellent strength and toughness because they carry chaotic arrangements of laths and a fine-grained interlocking microstructure, features that effectively divide PAGs into several subgrains and inhibit the propagation of cracks [35]. Fig. 2 presents a propagation path for a cleavage in steel grains with different microstructures [24,36]. Fig. 2(a) displays that in HSLA steels with low C_{eq}, FSPs and GBFs provide preferential crack propagation paths in grains due to the low dislocation density and similar crystal disorientation. The strength and toughness of steels are determined by the proportion of IAF in the microstructure [22,35,37–38]. As shown in Fig. 2(b), IAF is nucleated on the intragranular effective inclusions and presents chaotic orientation, resulting in the retardation of the initiation and propagation for a cleavage crack in the steel. In addition, the initially formed IAFs grow rapidly and divide the original austenitic grains into small areas. Later on, the IAFs grow only in these limited small areas so that the grains are divided into small sizes.

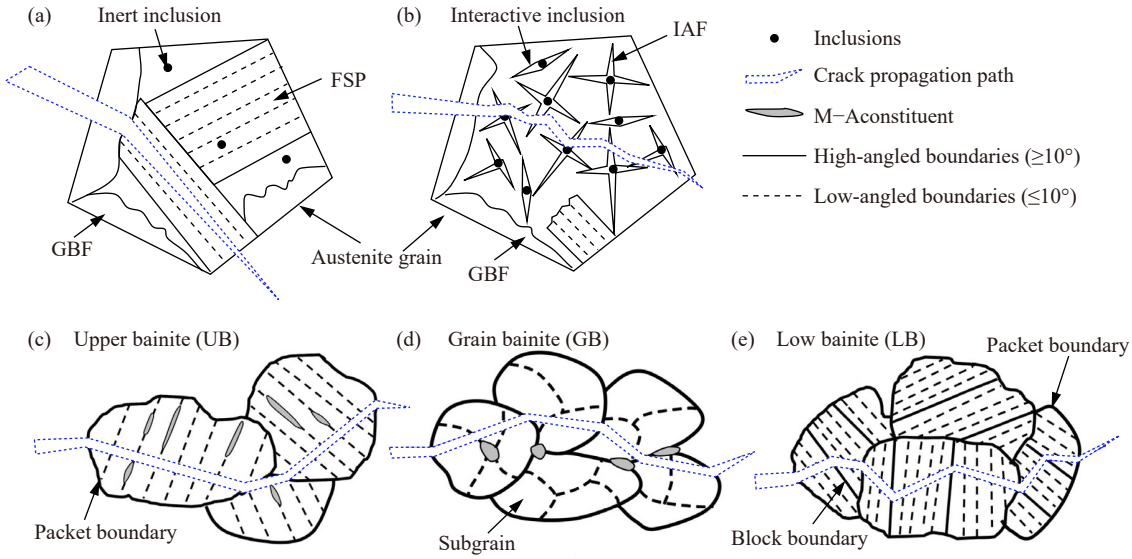

Fig. 2. Schematic of cleavage crack propagation paths in the steel grains with (a) FSP and (b) IAF microstructures; crack propagation paths in (c) UB, (d) GB, and (e) LB microstructures. (c–e) Reprinted by permission from Springer Nature: *Metall. Mater. Trans. A*, Correlation of microstructure and mechanical properties of thermomechanically processed low-carbon steels containing boron and copper, B. Hwang, C.G. Lee, and T.H. Lee, Copyright 2010 [36].

The bainite structure in the HAZ is relatively complex and varies with the austenite composition and transformation temperature. The microstructure is composed of several layers, including packet, block, and lath. Fig. 2(c)–(e) presents that in HSLA steels with high C_{eq}, the bainite can be classified into three categories depending on the presence or distribution of secondary phases such as M–A constituent and retained austenite (RA): UB, granular bainite (GB), and lower bainite (LB) [36]. GB consists of irregular ferrite structures and discrete islands of RA or M–A constituents. The microcrack easily formed at the boundaries between the M–A constituent and ferrite matrix and further propagated into the matrix when the concentrated stress exceeded the critical stress of the M–A constituent [22]. UB microstructures consist of parallel ferrite laths with largely mutual orientations separated by low-angle boundaries; meanwhile, cementite precipitates plenteously decorate the lath boundaries, which is detrimental to toughness [15,39]. Similar to UB, LB is a lath bainite arranged in parallel in lath shape. The main difference between them is the size and distribution of carbides. The carbides in UB are mainly cementite distributed between lath ferrites. Meanwhile, the carbides in LB are in the form of small dispersed sheets mainly found in the lath bainite, with a small amount in between the lath bainite structures. The effective grains of LB are relatively small, and the cracks are usually deflected by the high-angle grain boundaries (HAGBs) of LB; therefore, LB usually has a higher toughness than UB [36,40].

2.1.2. Mechanism of IAF nucleation induced by inclusions

Different points of view have been published on the mechanisms of IAF nucleation induced by inclusions. Although specific kinds of inclusions are essential for IAF nucleation, the exact mechanism by which inclusions induce IAF nucleation has not been identified, especially for multicomponent inclusions. According to published studies, four major mechanisms are responsible for IAF nucleation.

(1) Reduction of interfacial energy [41–42]. Inclusions act as inert substrates for the reduction of activation energy, and nucleation is controlled by the size, shape, and interfacial energy of the austenite/inclusion surface.

(2) Lattice mismatch mechanism [43]. A low lattice mismatch between ferrites and inclusions reduces the interfacial energy opposing nucleation.

(3) Solute depletion zone around nonmetallic inclusions [44]. This zone increases the thermodynamic driving force for the transformation from austenite to ferrite.

(4) Thermal strain mechanism [25,45]. As a result of differential thermal contraction between the austenite matrix

and the inclusion, the localized stresses may promote nucleation on dislocations local to the inclusion surface and/or increase the driving force for the transformation from austenite to ferrite.

In many cases, a single mechanism is not sufficient to explain IAF nucleation on inclusions. It is widely recognized that different mechanisms often work together to promote IAF nucleation on inclusions.

2.1.3. Effect of inclusions on IAF nucleation

IAF formation is the result of a succession of competing nucleation and growth processes at PAG boundaries and intragranular nucleation sites during cooling. Calculation results suggested that ferrite transformation begins at the austenite grain boundary sites because of the low free energy barriers to ferrite nucleation as transformation proceeds, and the intragranular inclusion sites should become operative [46]. IAF nucleation is affected by several factors, such as steel composition, PAG size, characteristics of nonmetallic inclusions, and cooling rate [33]. Under fixed chemical composition and welding method, nonmetallic inclusions influence IAF heterogeneous nucleation in the HAZ to a large degree [47]. Although inclusions provide external surfaces for IAF nucleation, some inclusions become inert because their characteristics, such as size distribution, number density, chemical compositions, and structure morphology, have different effects on IAF nucleation. Only inclusions with specific chemical compositions and structures can act as effective IAF nucleation sites.

In general, complex oxides are considered effective particles to induce IAF nucleation [38,48–49]. IAF nucleation may be independent of the underlying bulk compositions of the inclusions, and the surface compositions and inclusion structures actually have a decisive influence [50–51]. Wu *et al.* [52] indicated that the structures of inclusions and the behavior of MnS precipitation greatly affect IAF nucleation. Inclusions with MnS precipitation occurring in multiple local zones of the complex oxide surface are more conducive for IAF nucleation than simply wrapped ones. Some researchers confirmed that pure MnS cannot promote IAF nucleation around the inclusions, and even the thick MnS layer on the complex oxide may negatively affect IAF nucleation [53–54]. In addition, the inclusion's size markedly influences the IAF nucleation potency [23]. The nucleation rate expression has been deduced as follows to explain the mechanism of ferrite nucleation on the surface of inclusions [55]:

$$I_{\mathrm{I}} = f^{*} N_{\mathrm{I}} \exp\left(-\frac{\Delta G_{\mathrm{I}} + G_0}{k_{\mathrm{B}} T}\right) \propto \frac{1}{R_{\mathrm{I}}^3 (1-\cos\varphi)} \cdot \exp\left[-\frac{p\left(\frac{R_{\mathrm{I}}}{r_{\mathrm{c}}}, \theta\right) \Delta G_{\mathrm{H}}}{k_{\mathrm{B}} T}\right] \quad (1)$$

where I_{I} is the ferrite nucleation rate, f^{*} is the transition frequency of Fe, N_{I} is the potential nucleation position of ferrite on the surface of inclusion, G_0 is the grain boundary diffusion activation energy of Fe, k_{B} is the Boltzmann constant, T is the absolute temperature, R_{I} represents the radius of curvature of the inclusions, φ is a defined angle variable, p is an indicator that measures the difficulty of ferrite nucleation, r_{c} is the critical nucleation radius of ferrite formation on the surface of inclusion, θ represents the contact angle between the ferrite and inclusion, and G_{I} and G_{H} are the nuclear driving forces of ferrite formation on the surface of inclusion and homogeneous nucleation, respectively. Therefore, a theoretically optimal inclusion size exists, and the inclusions have a relatively high ferrite nucleation rate only within this range. Ricks *et al.* [42] confirmed that inclusions with sizes between 100 nm and 3 μm are beneficial to IAF heterogeneous nucleation. According to Barbaro *et al.* [56], IAFs are well nucleated when the nonmetallic inclusions are sized over 0.5 μm. Wu *et al.* [52] indicated that large numbers of complex inclusions with sizes between 0.5 and 3 μm are conducive to IAF heterogeneous nucleation. However, Yang *et al.* [34] indicated that inclusions larger than the critical size are only necessary but not sufficient. The critical size is also influenced by the inclusion's composition and crystal structure. Xu *et al.* [50] found that MgO–MnS complex inclusion with a size of 3.31 μm can function as the nucleation center of IAFs. Moreover, the number density of effective inclusions must be increased. The potency of IAF nucleation is proportionate to the number density of effective inclusions [57].

According to the discussion above, determining the effective surface compositions and increasing the number density of effective inclusions are vital to enhance IAF formation. Only inclusions with suitable characters can promote IAF nucleation.

2.1.4. Pinning effect of nanoparticles on the growth of austenite grains

During HHIW, the growth of PAGs is generally inhibited by the dragging force of the solute alloy elements segregated on the grain boundaries (solute drag) and the pinning force of fine particles, and the pinning force is much stronger than the dragging force [12,34,58–59]. The pinning effect of fine particles is schematically shown in Fig. 3 [31].

PAG coarsening affects the CGHAZ toughness because the presence of large austenite grains may lead to the formation of coarsened microstructures. The pinning force of particles is greatly controlled by the particle volume fraction and size, and the pinning effect of particles on austenite grain growth can be expressed by Zener's equation:

$$R = A \cdot \frac{r}{f} \quad (2)$$

where R is the radius of a PAG (μm), A is a constant, r is the radius of the secondary phase particles (μm), and f is the volume fraction of particles (%). From Zener's equation, the pinning effect of particles on grains in steel becomes stronger as the particle size decreases and the volume fraction of particles increases. When the target heating temperature increases, particle coarsening, dissolving, and reprecipitation take place and greatly affect the pinning force.

2.1.5. Proposal of oxide metallurgy technology

The properties of weld metals can be greatly improved if their microstructures are largely IAF [60]. In 1990, Takamura and Mizoguchi [61] introduced the concept of "oxide metallurgy," which makes use of the distributed small oxide

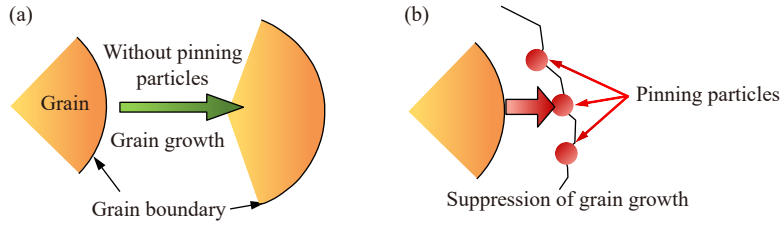

Fig. 3. Schematic of the pinning effect of fine particles. Reprinted from Ref. [31].

particles in the steel as beneficial phases, for the first time at the sixth International Iron and Steel Congress. Oxide metallurgy technology improves HAZ toughness from two aspects: one is to restrict the growth of PAGs using nanosized particles during the austenitizing stage of the steel to refine the grains, and the second is to induce IAF nucleation in the austenite grains to avoid the formation of GBF, FSP, and M–A constituent to refine the microstructures [15–16,62–64].

2.2. Industrial application of oxide metallurgy

Oxide metallurgy technologies were first applied in actual production by Nippon Steel Corporation, Japan (Nippon Steel), JFE Steel Corporation, Japan (JFE Steel), Kobe Steel, Ltd., Japan (Kobe Steel), and Baosteel Group Co., Ltd., China (Baosteel). Nippon Steel has long committed to utilizing oxide metallurgy to improve the HAZ toughness of steel, and the development process of this technology is presented in Fig. 4 [65]. In the early 1970s, fine and dispersed TiN particles were proposed to inhibit austenite grain coarsening during welding, and IAF was regarded as the optimum microstructure. However, TiN particles dissolve easily when the peak welding temperature exceeds 1400°C. Thereafter, Ti–O particles with a certain size were used to induce IAFs in the 1990s, and the interlocking IAF could also refine the grains in the welding HAZ. However, Ti_2O_3 easily aggregates and floats up in the molten steel; hence, the shape and size of Ti-containing inclusions in steel are not easy to control. After the year 2000, extensive studies have been conducted to develop an advanced oxide metallurgy technology utilizing strong deoxidizers, such as Mg, Ca, Zr, and REMs, which have a stronger affinity with oxygen than Al. Oxides or sulfides with these strong deoxidation elements can exist steadily even above 1400°C.

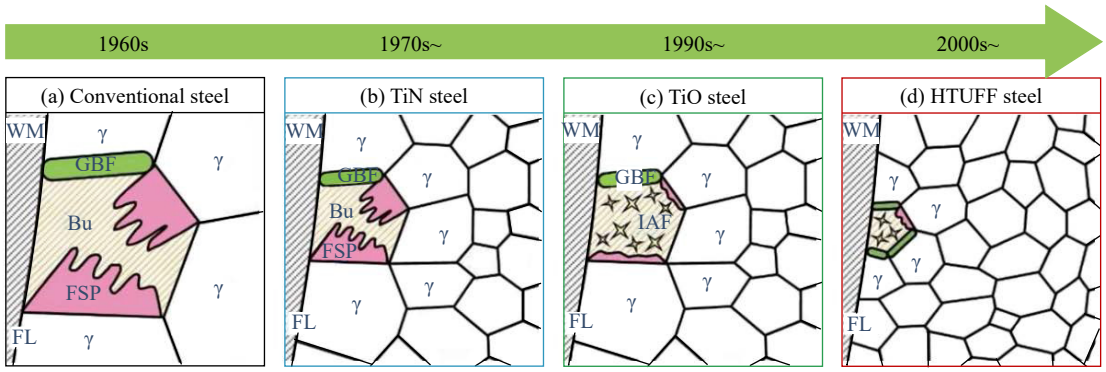

Fig. 4. Oxide metallurgy technology development in Nippon Steel Corporation. WM—weld metal; Bu—upper bainite; FL—fusion line. Reprinted from Ref. [65].

The successful industrial applications of oxide metallurgy include the super high HAZ toughness technology with fine microstructure imparted by fine particles (HTUFF) developed by Nippon Steel [65], the excellent quality in large heat input welded joins (EWEL) technique proposed by JFE Steel [66], the Kobe super toughness technology improved by the addition of Ca (KST) developed by Kobe Steel [67], and the excellent heat affected zone toughness technology improved by use of strong deoxidizers (ETISD) developed by Baosteel [16,68]. The detailed information is listed in Table 1.

3. Effect of deoxidation methods on oxide metallurgy technology

IAF formation is significantly governed by the deoxidation methods. Strong deoxidizers improve the microstructure and low-temperature toughness of the HAZ. The utilization of specific additives with strong affinities to O and S, such as Ti, Mg, Ca, Zr, REMs, and others, has been proven to effectively control nonmetallic inclusions and improve microstructures. Effective inclusions have also developed rapidly due to complex deoxidation.

3.1. Ti oxide metallurgy

Ti is widely used due to its ability to form stable oxides and nitrides even at high temperatures. Studies on Ti oxide metallurgy and the effect of Ti oxide on IAF nucleation were pursued in the early stage. Ti oxide is one of the most effective agents for IAF nucleation in Mn-containing steel and has been extensively investigated [45,69–72]. Obtaining Ti oxide or its compound oxides is the key to improving the weld-

Table 1. Introduction to the representative oxide metallurgy technologies

Year	Company	Technology	Technical key points	Application fields
2004	Nippon Steel	HTUFF [65]	(1) Mg and Ca are added into steel to form dispersed nanoparticles (10–100 nm). (2) These particles can strongly suppress the growth of PAGs. (3) Oxides and sulfides containing Mg/Ca are used to effectively induce IAF nucleation.	Structural steel with a tensile strength of 450–590 MPa, such as shipping building steel and pipeline steel
2005	JFE Steel	EWEL [66]	(1) Enhancing the pinning effects of TiN particles by optimizing the Ti/N ratio to control the grain size. (2) Adjusting the intragranular structure by optimizing the alloy compositions and controlling the contents of O, S, and Ca. (3) Using a super online accelerated cooling (Super-OLAC) process.	SA440 high-tensile-strength steel plates for architectural construction
2011	Kobe Steel	KST [67]	(1) Controlling the volume fraction of M–A constituent by utilizing a low C and low Si composition design. (2) Optimizing the Ti/N ratio to control the grain size. (3) Adjusting the contents of Ti and B to control the formation of Ti oxide and the segregation of B.	High-strength steel with a tensile strength of 780 MPa and a heat input of up to 400 kJ·cm^{-1}
2011	Baosteel	ETISD [16,68]	(1) Utilizing strong deoxidizers such as Mg, Ca, REMs, or Zr to control the formation of inclusions and precipitates. (2) The fine and dispersed TiN particles promoted by deoxidation with strong deoxidizers are utilized to pin the movement of the grain boundaries. (3) The dispersed oxides can effectively induce IAFs.	Shipbuilding steel plate for large container ship

ability of steels. Chai *et al.* [73] investigated the influence of Al and Ti on the nonmetallic inclusions and microstructures of CGHAZ in HSLA steel and found that the inclusions in Ti treatment steel mainly consist of Ti oxides and a small amount of Ti nitrides, both of which are beneficial to inducing IAF formation. Meanwhile, the inclusions in Al-treated steel mainly consist of Al oxides, which could not promote the formation of IAF microstructures.

Table 2 summarizes the typical Ti-containing inclusions that can effectively induce IAF nucleation [22,45,74–80]. These inclusions can be divided into two groups: (1) inclusions with Ti oxide as the core and MnS locally precipitated on the surface and (2) inclusions with Ti oxide as the core enwrapped by Ti carbonitrides. Mills *et al.* [80] found that TiO can induce IAF nucleation because it has a low misfit, with ferrites having a simple orientation. Most researchers believed that the typical inclusions, such as Ti_2O_3, in Ti-killed HSLA steels are favorable for IAF formation due to the generation of an MDZ around the inclusions [15]. Fig. 5(a) illustrates the typical inclusion of Ti_2O_3 with TiN and MnS precipitated on its surface and the heterogeneous nucleation for IAF on Ti_2O_3 inclusion, with an MDZ near the MnS wrapping around the Ti_2O_3 inclusion [79]. Shim *et al.* [81–82] demonstrated that many vacancies can be found inside a Ti_2O_3 particle, and Mn atoms are easily absorbed because of the similar radii of Ti^{3+} (0.069 nm) and Mn^{3+} (0.070 nm). Thus, an MDZ forms near the Ti oxides and increases the thermodynamic driving force for transformation from austenite to ferrite. This phenomenon explains why Mn is the indispensable element for Ti–O steel.

Table 2. Typical Ti-containing inclusions inducing IAF nucleation

Year	Authors	Inclusions	Nucleation mechanism	Location	Steel
2019	Shen *et al.* [22]	(Al,Ti,Mn)O_x–MnS	Mn-depleted zone	HAZ	HSLA steel
2016	Xuan *et al.* [74]	TiN–TiO_x–MnS	Mn-depleted zone; low lattice mismatch	Slab	HSLA steel
2015	Xiong *et al.* [75]	Ti_2O_3–MnS	Mn-depleted zone	HAZ	Low-carbon steel
2015	Seo *et al.* [76]	Ti_2O_3 and $MnTiO_3$	Mn-depleted zone	Weld metal	—
2014	Chai *et al.* [77]	Ti_2O_3–MnS	Mn-depleted zone	HAZ	Bearing steel
2009	Yamada *et al.* [78]	TiO	Low lattice mismatch	Weld metal	HSLA steel
2003	Byun *et al.* [45]	Ti_2O_3	Mn-depleted zone	Base metal	C–Mn steel
1996	Yamamoto *et al.* [79]	Ti_2O_3–MnS–TiN	Mn-depleted zone	HAZ	HSLA steel
1987	Mills *et al.* [80]	TiO–TiN	Low lattice mismatch	Weld metals	HSLA steel

Not all inclusions with Ti oxide as the core can induce IAF formation. According to Jiang *et al.* [83], in Ti–Al complex deoxidized HSLA steel, the IAF volume decreases with the rise of Ti and Al contents, as shown in Fig. 5(b)–(c), because the TiO_x–MnO oxide cores enwrapped by (MnO–SiO_2–Al_2O_3)–MnS or (MnO–SiO_2)–MnS surface layers are replaced by TiO_x–MnS, TiO_x–Al_2O_3, or Al_2O_3, which are weaker or impotent in inducing IAF. Shen *et al.* [22] studied the effect of Ti content on the precipitates in CGHAZ of HSLA steels subjected to 100 kJ·cm^{-1} heat input welding thermal cycle, and they indicated that the mean size and number density of precipitates in the low-Ti steel (0.012wt%

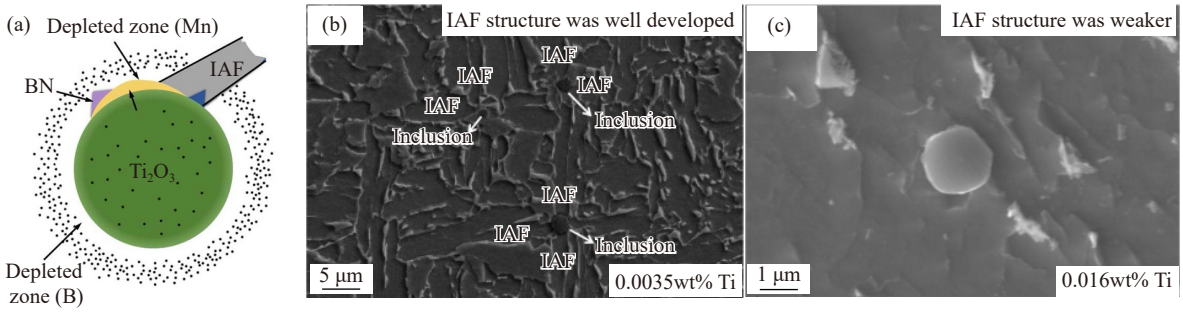

Fig. 5. (a) Schematic of precipitates on Ti_2O_3 and IAF formation in Ti-oxide bearing steels; microstructure observation of (b) typical IAF nucleation on inclusions in low-Ti steel and (c) ferrites nucleating on inclusions in high-Ti steel. (a) Reprinted with permission from Ref. [79]. © 1996 The Iron and Steel Institute of Japan. (b–c) Reprinted from *Mater. Charact*, 108, M. Jiang, X.H. Wang, Z.Y. Hu, K.P. Wang, C.W. Yang, and S.R. Li, Microstructure refinement and mechanical properties improvement by developing IAF on inclusions in Ti–Al complex deoxidized HSLA steel, 58-67, Copyright 2015, with permission from Elsevier [83].

Ti) are smaller and greater than those in the high-Ti steel (0.061wt% Ti), respectively. In the high-Ti steel, the PAG size in the CGHAZ also increases, the area fraction of IAF decreases, and the area fraction of the M–A constituent increases. As a consequence, the impact toughness of CGHAZ at −20°C decreases from 78 to 6 J with the increasing Ti content. This finding can be attributed to the inappropriate Ti/N ratio, leading to the formation of coarse TiN particles.

The Ti/N ratio should be optimized to deliver a sufficient density of TiN precipitates to retard austenite grain growth and avoid coarse TiN precipitates that are detrimental to the toughness performance. According to Medina *et al.* [84], a good grain size control can be achieved in the Ti/N weight ratio range of 2–4 as given in Fig. 6(a). Fig. 6(b) shows that at the near-stoichiometric Ti/N ratio, the high number density of precipitates in the simulated CGHAZ contributes to the fine austenite grain size and hence improves the CGHAZ toughness performance [85]. Rak *et al.* [86] studied the effect of Ti content on the precipitates in CGHAZ of offshore steel and reported that a Ti/N weight ratio of about 2.2 combined with the appropriate steel rolling processes is beneficial for uniformly dispersing fine TiN precipitates. The optimum Ti/N ratios are very different due to various discrepancies, such as in the alloy design and heat input of welding [87]. Furthermore, Kanazawa *et al.* [60] confirmed that the TiN phases are the effective nucleation sites for IAF formation. The precipitation of TiN on Ti_2O_3 contributes greatly to IAF nucleation because TiN has relatively high lattice coherency with ferrites, which decreases the interfacial energy of IAF nucleation on TiN [79,88].

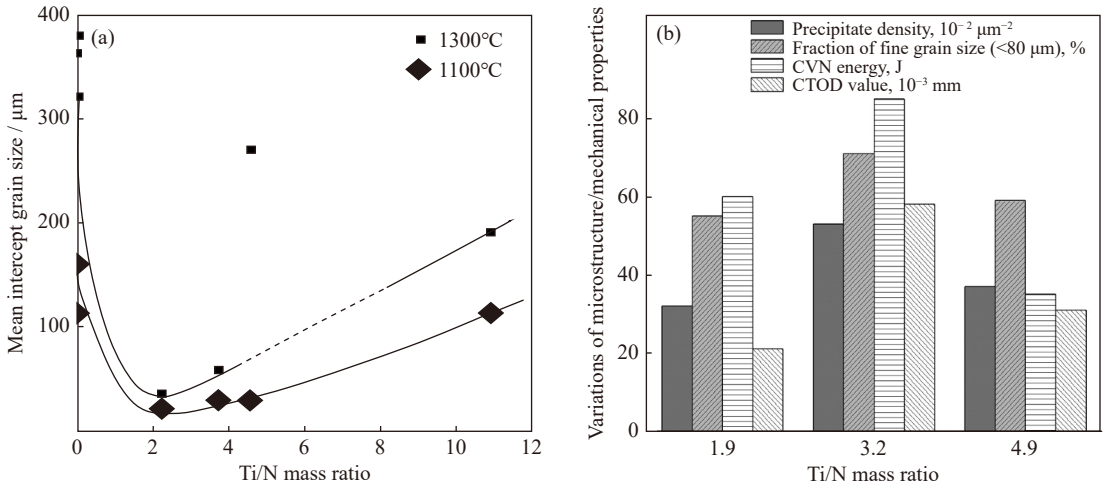

Fig. 6. (a) PAG size against the mass ratio of Ti/N at 1100°C × 10 min and 1300°C × 10 min for steels with N content of around 30–40 ppm; (b) variations of the precipitate density, fraction of fine grain sizes, Charpy V-notch (CVN) impact energy, and crack tip opening displacement (CTOD) value as a function of Ti/N mass ratio. (a) Reprinted with permission from Ref. [84]. © 1999 The Iron and Steel Institute of Japan. (b) Reprinted from *Mater. Des.*, 88, Z.X. Zhu, J. Han, and H.J. Li, Effect of alloy design on improving toughness for X70 steel during welding, 1326-1333, Copyright 2015, with permission from Elsevier [85].

Ti-alloyed steel is developed quickly because of the relatively low price of Ti and the stability of Ti_2O_3, even under high temperatures during welding [16,52]. However, Ti oxides have a tendency to grow up, and the desulfurization ability of Ti is not strong enough, so it is difficult to avoid a certain amount of pure MnS, which reduces the probabilities of IAF nucleation on inclusions [64,89–90]. Strong deoxidizers, such as Mg, Ca, Zr, or even REMs, which have a stronger affinity with oxygen than Al, are usually added with Ti to promote the dispersed distribution of fine-sized inclusions

[13,62,90–93]. In multiple microalloying steels with two or more alloying elements, the expected role of Ti becomes complicated due to the existence of Nb or V. The optimum Ti/N ratio should be low for steels containing additional microalloying elements (Nb or V) [86] because Nb and V also have a strong affinity with N to form NbN or VN. Thus, the oxide metallurgy technology for the steels containing Ti, Nb, and V is highly complex. The combination of Ti with other elements will be discussed in the following sections.

3.2. Mg oxide metallurgy

Mg-containing inclusions have attracted attention for the development of advanced oxide metallurgy [32,94–95]. Mg has a strong affinity with oxygen and sulfur than Al, so adding Mg to steel can easily produce fine inclusions, such as MgO–TiO_x, MgO–Al_2O_3, and MgO, which have been recognized as the most effective nuclei for IAF [93]. Mg-containing inclusions with size smaller than 0.1 μm, such as MgO-containing second-phase particles, inhibit austenitic grain growth in HAZ through the pinning effect; these particles have a lower binding force compared with the force between Al_2O_3 particles and have high thermal stability at temperatures higher than 1400°C [15,96]. Wang *et al.* [95] pointed out that Mg-containing inclusions cannot aggregate and appear as small dispersed particles because the disregistry between $MgAl_2O_4$ and MgO or Ti_2O_3 is very large. Zou *et al.* [97] discovered that in Mg-treated steel, the number of individual MnS particles decreases gradually after welding thermal simulation due to their precipitation on the surface of Ti–Al–Mg–O oxides, which is beneficial to inducing IAF.

Table 3 summarizes the typical inclusions inducing IAF in Mg-treated steel [49,54,62,94,97–102]. Wen *et al.* [101] simplified the Mg-bearing oxides as $MgAl_2O_4$ and attributed the nucleation-inducing effect to the low lattice mismatch between Mg-bearing inclusion and α-Fe. Kong *et al.* [103] proposed MDZ theory to explain the mechanism of how IAF nucleation is induced by Mg–Al–O inclusions in Mg-treated carbon structural steel. Hou *et al.* [104] used experiments and first-principles calculations to examine the interaction between Mn solute atoms and different oxides and found that Mn atoms can be absorbed into oxides by replacing the Mg in the crystal structures of $MgTi_2O_4$ and $MgTiO_3$. Therefore, the MDZ is generated by forming stable Mn–Ti complex oxides and/or by occupying the vacancies in Ti_2O_3 crystal. The MDZ theory still plays an important role in explaining IAF nucleation in Mg deoxidization steel.

Table 3. Typical Mg-containing inclusions inducing IAF nucleation

Year	Authors	Inclusions	Nucleation mechanism	Location	Steel
2020	Our previous work [94]	MgO–Ti_2O_3–MnS	—	HAZ	Shipbuilding steel
2019	Zou *et al.* [97]	Al–Mg–Ti–O–MnS	Mn-depleted zone	HAZ	EH36 shipbuilding steel
2019	Liu *et al.* [98]	Al–Ti–Mg–MnS	Mn-depleted zone	HAZ	HSLA steel
2018	Our previous work [49]	MgO–Al_2O_3–Ti_2O_3–MnS	Mn-depleted zone	HAZ	Shipbuilding steel
2018	Lou *et al.* [99]	Ti–Ca–Mg–O–MnS	Mn-depleted zone	HAZ	HSLA steel
2018	Wang *et al.* [62]	Al_2O_3–MgO–Ti_xO_y–Nb(C,N)	Low lattice mismatch	HAZ/ingot	Shipbuilding steel
2018	Tian *et al.* [54]	Mg–Al–O–Si–Mn–S	Mn-depleted zone	Ingot	Carbon structural steel
2017	Our previous work [100]	MgO–MnS	—	HAZ	High-strength thick steel plates
2011	Wen *et al.* [101]	$MgAl_2O_4$, MgO	Low lattice mismatch	Ingot	SiMg steel
2009	Chai *et al.* [102]	Mg–Ti–O	—	HAZ	Ti-killed steel

Mg treatment also promotes TiN precipitation. Sun *et al.* [96] revealed the effect and mechanism of Mg on the nanoscale pinning particles in the HAZ of shipbuilding steel. When the heat input of welding is <250 $kJ·cm^{-1}$, the number of particles between 40 and 120 nm is constant because the generated MgO delays the solid solution of TiN. Our previous work [37,94,105] reported the evolution of inclusions, precipitates, and HAZ microstructures in shipbuilding steel after HHIW and found that with the increase in Mg content from 0 to 0.0099wt%, the phase of central oxide inclusions changes sequentially from Al_2O_3 to (Mg–Ti–O). In addition, MgO, the major microstructure in the HAZ, changes from FSP, UB, and GBF to IAF, with the austenite size decreasing from 437 to 122 μm as presented in Fig. 7(a)–(d). Owing to the strong affinity ability of Mg with oxygen, the deoxidation products of Ti are easily reduced by Mg, promoting the dissolution of Ti element in steel. The superabundance of Ti in steel can combine with N to form fine TiN particles after the molten steel has solidified. Therefore, with the increasing Mg content from 0 to 0.0044wt%, the number of TiN particles per unit volume increases, and HAZ toughness is improved significantly, as plotted in Fig. 7(e) and (f).

Mg usually plays an important role in sufficiently dispersing the inclusions. Adding Mg can refine the Ti_2O_3 inclusions in molten steel by modifying them into Mg-containing complex inclusions, which are small and difficult to polymerize [96]. The strong affinity of Mg with oxygen is beneficial for the precipitation of fine dispersed TiN particles, providing strong pinning effects for inhibiting grain growth at high temperatures. The application of Mg treatment is limited to some extent because the high vapor pressure of Mg makes it difficult to add to molten steel and thus easily removed by boiling and evaporation [62]. Therefore, Mg treatment is usually combined with Ti treatment to increase the yield. The addition of microalloying elements in the order of Al, Mg, Ti is the key to obtaining abundant dispersion and fine nucleation in austenite [95,106]. If MgO is formed at the right moment, then the aggregation of Al_2O_3 and Ti_2O_3 can be

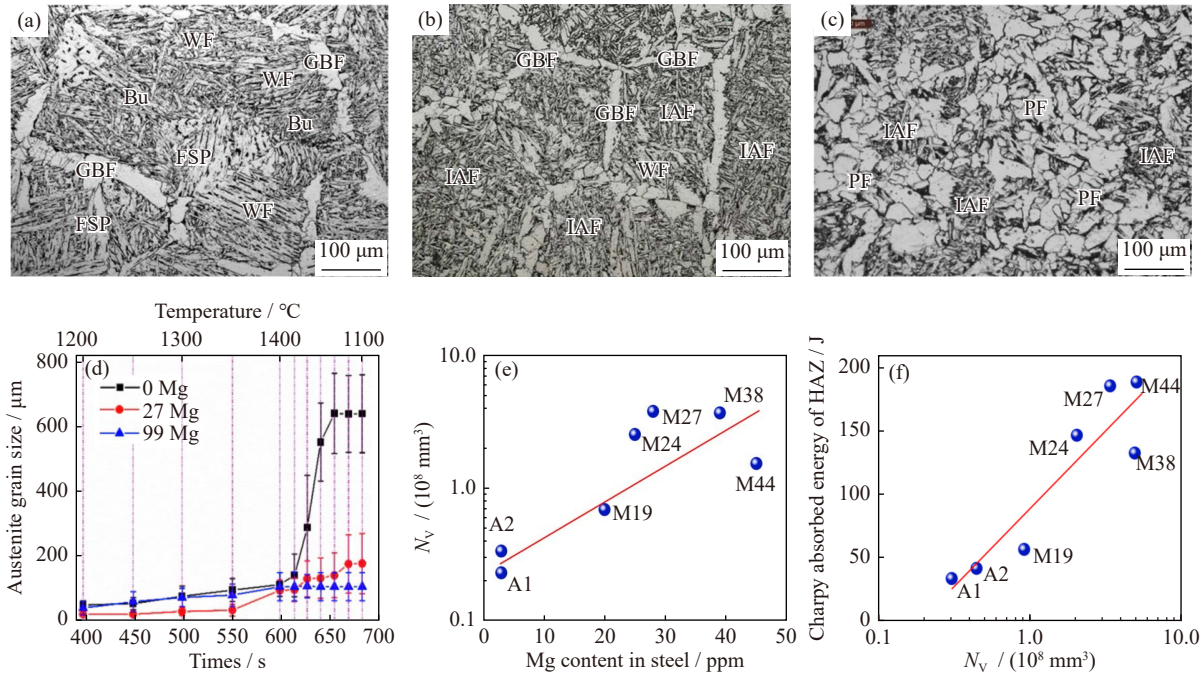

Fig. 7. Effect of Mg on the microstructures, PAG size, and pinning particles: (a–c) typical microstructure of (a) M0, (b) M27, and (c) M99; (d) changes in the average PAG size with temperature or residence time in the high-temperature laser scanning confocal microscopy observation; (e) relation between the number of nanoscale TiN particles per unit volume (N_V) and Mg content in the steel; (f) relation between N_V and HAZ toughness (M*x* represents the steel with *x* ppm addition of Mg element; A1 (0.0022wt% O) and A2 (0.0033wt% O) are steels without Mg addition). (a–c) Reprinted by permission from Springer Nature: *Metall. Mater. Trans. A,* Effect of Mg content on the microstructure and toughness of heat-affected zone of steel plate after high heat input welding, L.Y. Xu, J. Yang, R.Z. Wang, Y.N. Wang, and W.L. Wang, Copyright 2016 [37]. (d) Reprinted from Ref. [94]. (e, f) Reprinted by permission from Springer Nature: *Metall. Mater. Trans. A.,* Effects of Mg content on characteristics of nanoscale TiN particles and toughness of heat-affected zones of steel plates after high-heat-input welding, L.Y. Xu and J. Yang, Copyright 2020 [105].

weakened and replaced by fine and dispersed composite oxides [62].

3.3. Ca oxide metallurgy

In addition to Mg, Ca is another strong deoxidant and has a great affinity with sulfur [1]. In recent years, oxide metallurgy with Ca deoxidation has been intensively studied [88,107]. Table 4 summarizes the typical works on Ca-containing inclusions that induce IAF formation [13,15,38,48,107–110]. Ca-oxysulfide has a good coherency with ferrites, which is effective in promoting IAF nucleation [108,110]. Wang *et al.* [109] confirmed that Ti–Ca–Al–Mn–S oxides with the appropriate size of 0.3–2 μm in the HAZ of Ti–Ca killed HSLA steel can effectively promote IAF nucleation and remarkably improve HAZ toughness.

Table 4. Typical Ca-containing inclusions inducing IAF nucleation

Year	Authors	Inclusions	Nucleation mechanism	Location	Steel
2021	Liu *et al.* [108]	Ca–Mg–Al–O + MnS/MnS–CaS	Mn-depleted zone	Ingot	EH36 steel
2020	Wang *et al.* [13]	Ti–Ca–O–Mn–S	Mn-depleted zone	HAZ	HSLA steel
2020	Wang *et al.* [109]	Ti–Ca–Al–Mn–S oxides	Mn-depleted zone	HAZ	HSLA steel
2020	Wang *et al.* [38]	TiO_x–CaO–Al_2O_3–MnS	Mn-depleted zone	HAZ	HSLA steel
2019	Our previous work [107]	(CaS–)MnS–Al_2O_3–CaO–Ti_2O_3	Mn-depleted zone	HAZ	HSLA steel
2018	Terazawa *et al.* [48]	(Al–Ca–O)–CaS	Low lattice mismatch	HAZ	Low-carbon steel
2018	Lou *et al.* [15]	TiO_x–Ca(O,S)–MnS	Thermal strain energy	HAZ	Low-carbon steel
1995	Lee and Pan [110]	Ti–Ca-oxysulfides	Low lattice mismatch Thermal strain energy	HAZ	Ti-killed steel

The effects of Ca content on the evolution of inclusions and precipitates in steels have been systematically studied recently. Ca can reduce Ti oxide to form the dissolved Ti in liquid steel. Thus, the content of Ti in molten steel is affected by Ca addition [111]. According to Kato *et al.* [67] from Kobe Steel, TiN crystallizes preferentially on Al_2O_3 particles but not on CaS or CaO–Al_2O_3 particles due to the large lattice misfit and critical nucleus formation energy. Therefore, the crystallization of coarse TiN particles is inhibited, and the number of fine TiN particles increases after Ca addition. In our previous work, the inclusion characterization, precipitates, and microstructures in steel with different Ca contents

were investigated [1,107,112]. The results show that with the increasing Ca content from 0.0002wt% to 0.0025wt%, the quantity of pure MnS particles significantly decreases, but that of complex oxysulfide particles (which can promote IAF formation) increases. In addition, the coarse FSP is eliminated, as presented in Fig. 8(a)–(d). As pictured in Fig. 8(e) and (f), the precipitations of TiN particles greater than 50 nm and smaller than 50 nm are promoted by Ca addition, effectively preventing grain growth. As a consequence, HAZ toughness is substantially enhanced.

Ca treatment is a well-established method to modify solid inclusions. Owing to the strong affinity of Ca with oxygen and sulfur, Ca-oxysulfide is easy to form and is beneficial for reducing individual MnS precipitates and promoting IAF nucleation. Although Ca oxide metallurgy technology can facilitate the formation of fine TiN particles, its grain refinement effect is not as obvious as that of Mg treatment. Promoting IAF formation can be considered the most important contribution of Ca oxide metallurgy for improving the HAZ impact toughness. One of the problems for Ca oxide metallurgy is that Ca has a relatively low yield in the molten steel due to its high vapor pressure and low boiling point (1484°C). Therefore, Ca has always been added with Ti to refine grains in steels and to improve the strength and toughness of steel welds.

3.4. Zr oxide metallurgy

As a congener of Ti, Zr has many similar properties to Ti. The density of ZrO_2 is close to that of steel, allowing it to easily form uniformly dispersed inclusions. The treatment of Ti-bearing steel with Zr can refine and modify the Ti oxides [34,113]. Table 5 summarizes the typical work on IAF nucleation in Zr-bearing steel [11,20–21,47,97,114–118]. In general, the modified Ti–Zr complex oxides become the nucleation core of MnS [21,119]. Zr-containing compound inclusions are considered effective nucleation sites for IAF because of the formation of MDZ. According to Li *et al.* [117], the diffusion of Mn into ZrO_2 and the formation of ferrite within the MDZ in the vicinity of ZrO_2 can be proven by experiments and first-principles calculations.

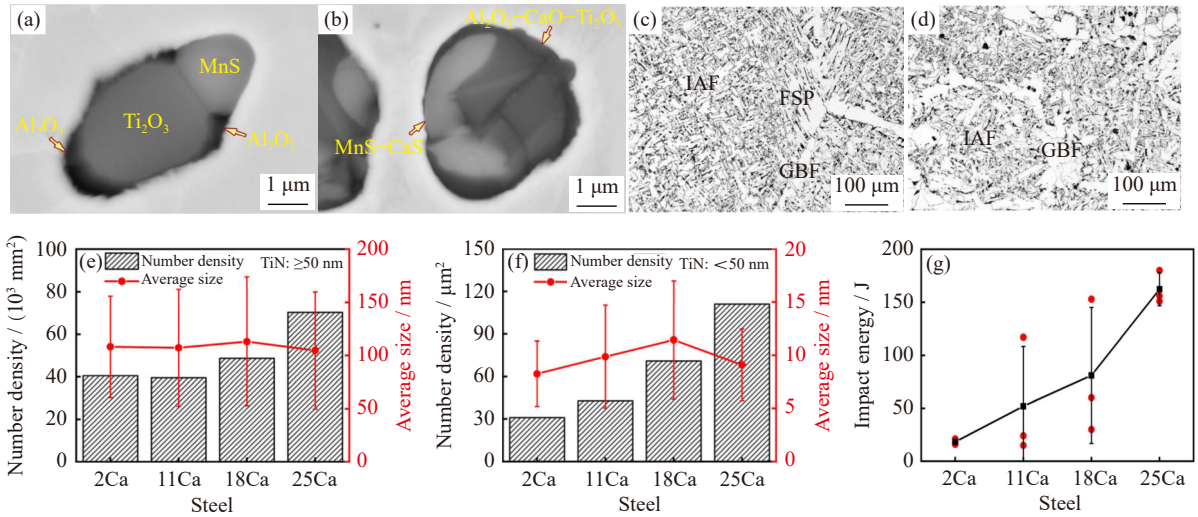

Fig. 8. Effect of Ca addition on the CGHAZ in HSLA steels: scanning electron microscope (SEM) images of typical inclusions in (a) 2Ca and (b) 25Ca steels; microstructures of (c) 2Ca and (d) 25Ca steels; number density and average size of TiN particles (e) greater than 50 nm and (f) smaller than 50 nm; (g) impact toughness of the CGHAZ at −20°C. (*x*Ca represents the steel with *x* ppm addition of Ca element). (a–d) Reprinted from Ref. [1]. (e–g) Reprinted by permission from Springer Nature: *Metall. Mater. Trans. A.*, Improvement of impact toughness of the welding heat-affected zone in high-strength low-alloy steels through Ca deoxidation, Y.H. Zhang, J. Yang, D.K. Liu, X.Q. Pan, and L.Y. Xu, Copyright 2021 [112].

Table 5. Typical Zr-containing inclusions inducing IAF nucleation

Year	Authors	Inclusions	Nucleation mechanism	Location	Steel
2023	Liu *et al.* [114]	Ti–Zr–O + MnS	Mn-depleted zone	HAZ	Low-carbon steel
2022	Liu *et al.* [115]	$CaO–Al_2O_3–TiO_x–ZrO_2–MnS$	Mn-depleted zone	HAZ	Shipbuilding steel
2020	Wang *et al.* [47]	(Ti,Ca,Zr,Al)–O–Mn–S	Mn-depleted zone	Ingot	Low-carbon steel
2019	Liu *et al.* [11]	Zr–Al–Ti–O–MnS	Mn-depleted zone	HAZ	HSLA steel
2019	Zou *et al.* [97]	Zr–O–Mn–S–Ca–Mg	Mn-depleted zone	HAZ	EH36 shipbuilding steel
2018	Zou *et al.* [116]	Zr–O–Ti–Ca	—	Rolled plate	EH36 shipbuilding steel
2016	Zhou *et al.* [20]	Zr–Ti oxide	Mn-depleted zone	HAZ	EH36 shipbuilding steel
2014	Li *et al.* [117]	ZrO_2	Mn-depleted zone	—	HSLA Steel
2010	Ma *et al.* [118]	$MgO–ZrO_2–TiO_x–MnS$	—	HAZ	Low-carbon Steel
2008	Guo *et al.* [21]	$ZrO_2–MnS$	Mn-depleted zone	HAZ	HSLA pipeline steel

Investigation results on Zr addition show that Zr oxides can induce IAF nucleation and effectively refine austenite grains. Guo *et al.* [21] reported that Zr addition improves the impact toughness of the HAZ in HSLA pipeline steel because of the formation of ZrO_2–MnS, which can facilitate IAF formation. Thermochemical data indicate that, similar to Ti, Zr is a strong nitride-forming element. ZrN can retard austenite grain growth during reheating because ZrN is a high-melting-point compound [21]. Zhou *et al.* [20] observed and investigated the grain refinement of HAZ in HSLA steels with Zr–Ti combined deoxidation and found that a large amount of fine Zr–Ti oxide particles are formed in the steel and retard the austenite grain growth during the simulated welding thermal cycle. Liu *et al.* [11] investigated the effect of Zr addition on the microstructure and impact toughness in the CGHAZ of HSLA steels subjected to 100 kJ·cm^{-1} heat input and discovered that Al–Ti complex oxides and (Ti,Nb)N precipitates in Zr-free steel are transformed into fine Zr–Al–Ti complex oxides and (Al,Ti,Nb)N precipitates in Zr-bearing steel as presented in Fig. 9. The dissolved Al and Ti contents (in liquid steel) are increased by the reduction of Al and Ti oxides through the dissolved Zr, which is conducive to the precipitation of Al and Ti nitrides in Zr-bearing steel. As illustrated in Fig. 9(b), the grains in the CGHAZ of the Zr-bearing steel are smaller and more uniform than those in the Zr-free steel, and the area fraction of IAF in the Zr-bearing steel is 2.5 times greater than that in the Zr-free steel. As a consequence, the impact toughness is significantly improved by Zr addition.

Owing to the formation of MDZ in the vicinity of ZrO_2, Zr deoxidation greatly improves IAF transformation and strongly prevents coarse intergranular structures. This finding proves that Zr enhances the impact toughness of HSLA steel. However, one study compared the nucleation behavior of ferrites induced by inclusions in the HAZs of EH36-Mg and EH36-Zr shipbuilding steels and found that Al–Mg–Ti–O–Mn–S provides more effective ferrite nucleation sites than Zr–O–Mn–S–Ca–Mg [97]. This result indicates that a larger driving force is required for the Zr–O–Mn–S–Ca–Mg transformation. In addition, Zou *et al.* [116] found that the IAF nucleates on the surface of Zr-containing inclusions in the Zr-deoxidized EH36 rolled plate; however, in the simulated welding samples, the inclusions are almost ZrO_2, and the IAF structure is hardly detected.

3.5. REM oxide metallurgy

REMs exhibit strong abilities to modify inclusions and improve the properties of steels. The spherical high-melting-point REM oxides and REM sulfides, such as $REAlO_3$, RE_2O_3, and RE_2O_2S, in liquid steel can effectively act as nucleation sites for IAF [90,120]. Table 6 summarizes the typical works on REM-containing inclusions inducing IAF nucleation [90,111,120–124]. These REM inclusion compounds usually have a low mismatch with ferrite, which promotes IAF nucleation. In many cases, an MDZ around Ce-containing inclusion is difficult to find. The RE_2O_2S and RE_2S_3 in steel are more prone to induce IAF formation than $REAlO_3$ because the lattice misfit between RE_2O_2S/RE_2S_3 and ferrites is much smaller than that between $REAlO_3$ and ferrites.

REMs also play an important role in grain refinement. REM-containing inclusions with high melting points can pin the grain boundary movement during heating [111]. REMs

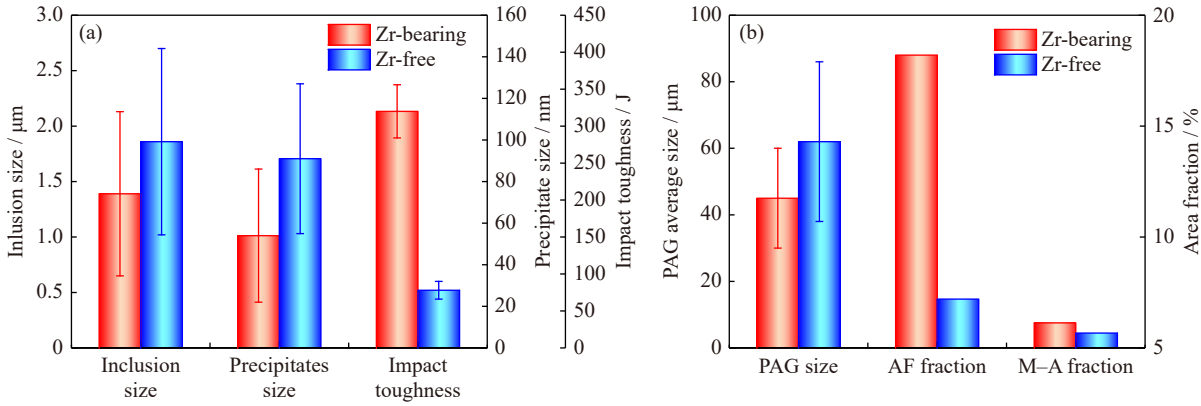

Fig. 9. Effect of Zr addition on the CGHAZ in HSLA steels: (a) average sizes of inclusions and precipitates and the impact toughness; (b) PAG size and area fractions of IAF and M–A constituent. Data source from Ref. [11].

Table 6. Typical REM-containing inclusions inducing IAF nucleation.

Year	Authors	Inclusions	Nucleation mechanism	Location	Steel
2021	Cao *et al.* [120]	Ce_2O_2S	Low lattice mismatch	HAZ	HSLA steel
2020	Liu *et al.* [90]	Ce_2O_2S–MgO–MnS	Low lattice mismatch	Ingot	EH36 steel
2019	Cao *et al.* [121]	Y_2O_2S	Low lattice mismatch	HAZ	X70 pipeline steel
2019	Cao *et al.* [111]	$CeAlO_3$–TiN	Low lattice mismatch	HAZ	Pipeline steel
2019	Song *et al.* [122]	La_2O_2S–MnS	Mn-depleted zone;low lattice mismatch	HAZ	C–Mn steel
2015	Nako *et al.* [123]	Ti–Zr–REM oxides	Low lattice mismatch	HAZ	Low-carbon steel
2006	Thewlis [124]	Ce-sulfide	Low lattice mismatch	Ingot/HAZ	Low-alloy steel

tend to segregate to austenite grain boundaries during the thermal cycle of CGHAZ, thus suppressing FSP transformation and promoting IAF transformation [30,125]. The segregation of REM atoms at the grain boundaries also reduces the boundary energy and surface tension, leading to a reduction in the driving force for grain growth [2]. Cao *et al.* [120] investigated the Ce content on the particle characteristics in CGHAZ after HHIW at 100 kJ·cm^{-1} for HSLA steels and found that the number densities of inclusions and precipitates increase with the Ce content from 0.012wt% to 0.086wt% as presented in Fig. 10(a)–(b), and the impact energy is decreased from 105 to 24 J. The average PAG sizes decrease, and a high fraction of IAF is formed in the 0.012wt% Ce-treated steel because of the low mismatch between Ce_2O_2S and α-Fe, as shown in Fig. 10(c)–(f). Therefore, the superior impact toughness in the CGHAZ of the 0.012wt%Ce steel is attributed to the higher fraction of IAF and the lower fraction of M–A constituent compared with those in the other treated steels.

Compared with Mg or Ca treatment, REMs possess a higher boiling point (higher than 3000°C) and a higher yield [29–30,92]. However, some problems remained to be addressed for their industrial production. On the one hand, REM treatment is always accompanied by submerged nozzle clogging. On the other hand, the range of compositions possible for Ce-alloyed steels is very narrow for obtaining active inclusions. Therefore, REM–Ca or REM with Ti or Mg treatment should be studied so that optimized refining, and the application of REM oxide metallurgy technology can be achieved.

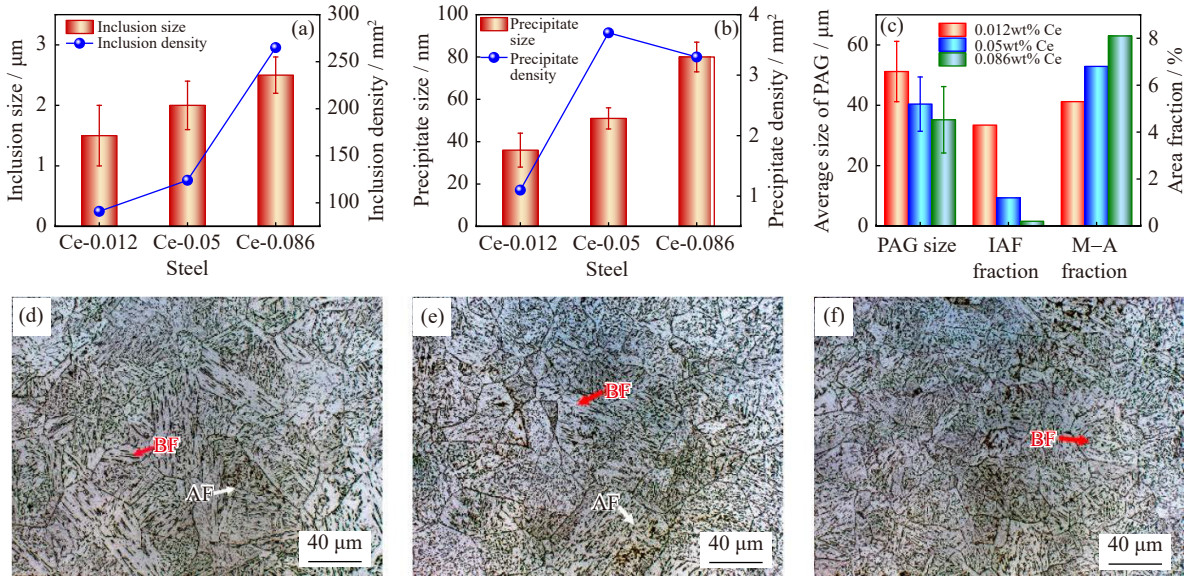

Fig. 10. Effects of Ce on the CGHAZ in the investigated steels: sizes and densities of (a) inclusions; (b) precipitates, and (c) PAG size and fractions of IAF and M–A constituent; SEM micrographs of (d) 0.012wt%Ce steel, (e) 0.05wt%Ce steel, and (f) 0.086wt%Ce steel, respectively. BF—bainite ferrite; AF—acicular ferrite. Reprinted from Ref. [120].

4. Effect of microalloying elements on oxide metallurgy

At present, studies on oxide metallurgy are no longer limited to the role of single oxides and sulfides on IAF nucleation and instead focus on the role of composite inclusions comprised of oxides, sulfides, and carbonitrides. Oxides formed by deoxidant elements with carbonitrides or sulfides precipitated thereon also have a profound influence on IAF nucleation [14,95,126]. In addition, carbides or nitrides formed by microalloying elements are effective particles in inhibiting the motion of grain boundaries during welding. For the microalloying system of HHIW steel produced by oxide metallurgy technology, the synergistic mechanism of various microalloying elements, such as C, Si, Nb, V, Cr, Mo, and B, must be studied.

4.1. Effect of C, Si, and Al

C, Si, and Al are the elements in HSLA steels necessary to ensure the sufficient tensile strength of base metal and affect the formation of the M–A constituents and cementite of HAZ. However, the influence of their contents on the HAZ microstructures in steel plates for HHIW has not been comprehensively investigated.

C is one of the basic interstitial solutes that enhance the strength of steel. During welding, the C content has the most obvious effect on HAZ toughness. The increase in C content can enhance the HAZ hardness but reduce the ductility and toughness of the HAZ [29]. When the C content increases, IAF is replaced by some brittle microstructures that seriously deteriorate the HAZ impact toughness. Mu *et al.* [127] stated that the potency of IAF formation on inclusions in Fe–C alloys decreases with the increase in C content due to the large amount of pearlite formation in steels with a high C content. The C depletion zone around the inclusion surface promotes IAF formation [128]. In addition, C easily forms carbides with other alloying elements, especially in HSLA steels with complex alloying elements. Kim *et al.* [129] studied the ef-

fect of alloying elements on the fracture toughness in the HAZ of Mn–Mo–Ni-alloy steel and revealed that with the decrease of C content and the increase of Mo and Ni contents, the number of fine M_2C (M represents metal elements) greatly increases and the number of coarse M_3C decreases, leading to the simultaneous improvement of tensile properties and fracture toughness. In our previous study [130], we investigated the combined effect of C and Si contents on the microstructure and low-temperature impact toughness of the HAZ of offshore engineering steel with Ca deoxidation, and the results showed that high C and Si contents promote the precipitation of $M_{23}C_6$ and cementite but restrain the formation of MC and M_2C. When the C and Si contents decrease, the microstructure becomes significantly refined, leading to an improvement in HAZ toughness. The low C content in HSLA steel improves its weldability, under the same welding conditions but a certain amount of alloying elements is added to compensate for the loss of steel strength, which represents high C_{eq}.

Si is also an alloying element frequently added to HSLA steel, for it can notably improve the steel strength through solid solution strengthening. Si addition notably improves the steel strength through solid solution strengthening. However, excessive Si can promote C enrichment in austenite and, accordingly, the stabilization of RA, which further transforms to island M–A constituents and degrades the impact toughness [131]. The effect of Si content on HAZ toughness of offshore engineering steels with Mg or Ca deoxidation was confirmed in our previous industrial tests and laboratory studies [32,130]. The HAZ toughness at −40°C is decreased from 202 to 58 J with increasing Si content. Fig. 11(a)–(e) presents that with the increasing Si content, the shapes of M–A constituents transform from dotted and filmed ones to the coarsened stringer and blocky ones that tend to initiate cracks in HAZ, which leads to a decrease in HAGBs. Increasing the Si content also raises the transformation temperature of austenite to ferrite, providing a low supercooling rate degree and enabling the formation of the mixed GB + LB microstructures in the high-Si steel. Therefore, the CGHAZ microstructures are transformed from fine and interlocked LBs into coarsened LBs and small amounts of GBs, reducing the energy for the propagation of cracks.

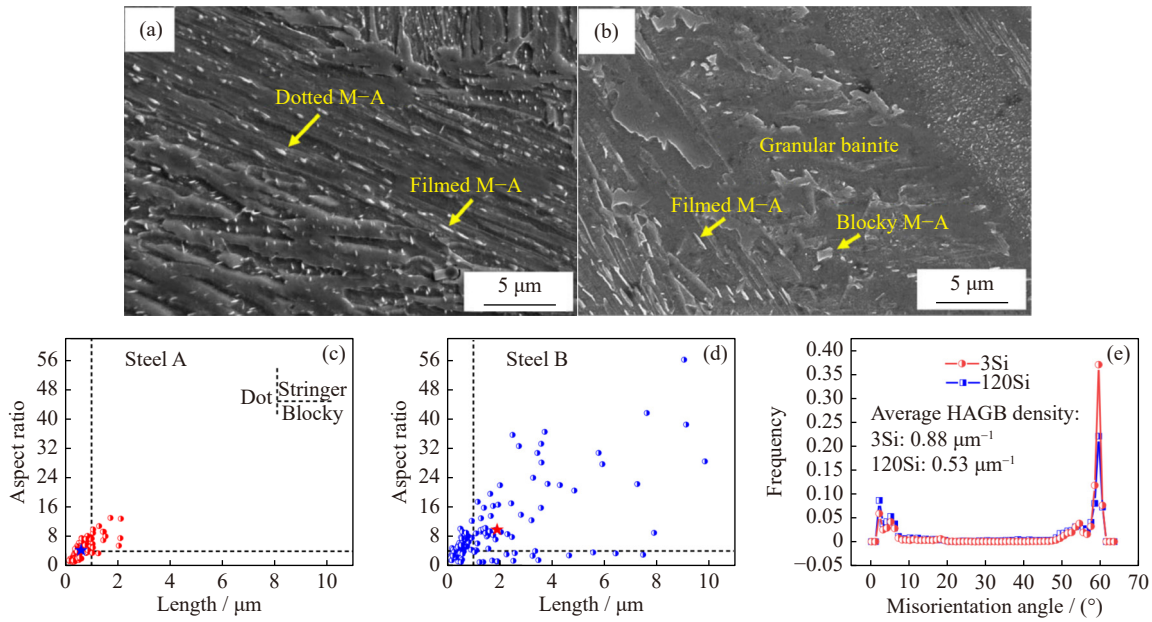

Fig. 11. Effect of Si on CGHAZ in HSLA steels: SEM morphologies of CGHAZ microstructures in (a) 3Si and (b) 120Si steels; individual values of the length and aspect ratio (length/width) for randomly selected 150 M–A constituents and the average values noted by the star signs in (c) 3Si and (d) 120Si steels; (e) frequency distributions of boundary misorientations (3Si and 120Si means the two steels with 0.003wt% Si and 0.120wt% Si, respectively). X.Q. Pan, J. Yang, Y.H. Zhang, and R.B. Li, *Steel Res. Int.*, vol. 94, art. No. 2200534 (2023) [32]. Copyright Wiley-VCH Verlag GmbH. Reproduced with permission.

Al can be added in small quantities to assist fine grain formation in microalloying steel. Since Al forms nitrides with nitrogen, it is used as an alloying element in steels. For steels using oxide metallurgy, the Al content seriously affects the effectiveness of the oxide metallurgy, because the Al element has a good chemical attraction to oxygen. Wu *et al.* [52] systematically investigated the effect of Al on the IAF nucleation in HSLA steel slabs with Al–Ti–Mg deoxidation. They revealed that the inclusions in steels with low Al content are conducive to the precipitation of multiple thin manganese sulfides on the local surfaces of Al-containing inclusions, which is beneficial for inducing IAF nucleation. In our previous works, the influence of Al content on the submicron particles, nanoparticles, PAG size, and inclusion–microstructure relationship in the HAZ of Mg-deoxidized steel was studied [50,132–133]. The results showed that the micron-inclusions in two steels containing different Al contents exhibit diverse morphologies with different nucleation abilities for IAFs, as shown in Fig. 12. The inclusions in the HAZ with lower Al content are likely to induce IAF nucleation. Therefore, a high Al content is not conducive to the impact toughness of HAZ with Ti–Mg deoxidation steel. Whether the Al

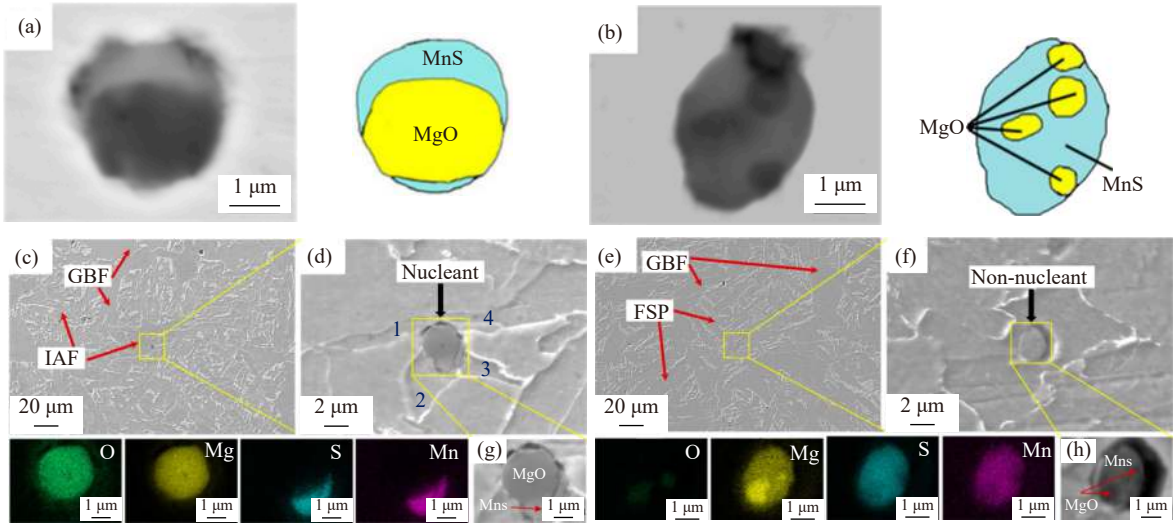

Fig. 12. Effect of Al addition on the HAZ: morphologies and compositions of typical inclusions in steels with (a) low-Al and (b) high-Al contents; morphologies and SEM mapping images of inclusions in HAZ microstructures for steels with (c–d, g) low-Al and (e–f, h) high-Al contents. Reprinted from Ref. [50].

content has the same effect on the HAZ of HSLA steel with Ca, Zr, or REM deoxidation remains unclear.

4.2. Effects of Nb and V

Nb and V are strong carbide-forming elements. Small additions of Nb and V, individually or in combination, enhance the steel strength for two reasons. First, the formation of microalloy carbides and nitrides with a size smaller than 0.1 μm helps restrict grain growth during welding so that the PAGs are refined [133–134]. Second, some carbonitrides are effective sites for IAF nucleation [106,126].

Nb has been widely applied to enhance steel strength by precipitation and grain refinement. Its addition also improves the hardenability of steel [109]. Microalloying with Nb is beneficial in improving the impact toughness of HAZ. However, the pinning effect of Nb precipitates on the austenite grain boundary is restricted to peak temperatures below about 1100°C [86]. Nevertheless, the peak temperature of HAZ during HHIW is even greater than 1400°C; that is, most of the fine Nb(C,N) precipitates in the matrix will dissolve during welding. Moon *et al.* [135] found that compared with TiN particles, the high-temperature stability of the complex (Ti,Nb)(C,N) particles formed by Nb addition deteriorates, thereby coarsening the particles and austenite grains. At present, the effect and mechanism of Nb addition on TiN particles and austenite grain growth during continuous cooling are still under discussion, especially for oxide metallurgy steel. Our previous studies concluded that increasing the Nb content decreases the toughness of HAZ after HHIW at 400 kJ·cm^{-1} for shipbuilding steel plates with Mg/Ca deoxidation [136–137]. Increasing the Nb content also influences the coarsening and thermostability of TiN precipitates during the welding thermal cycle due to the transformation of particles from TiN to (Ti,Nb)(C,N), leading to the growth of PAGs as illustrated in Fig. 13(a) and (b). Yang *et al.* [138] also pointed out that the Ti/Nb precipitates in the CGHAZ of Ti deoxidation steel with a high Nb content are coarse and cumulate (Fig. 13(c)) and thus are responsible for the abnormal growth of PAGs, which is not conducive to the impact performance. Nb addition also hinders the ferrite transformation and decreases the content of IAFs. Therefore, the decrease in the high-temperature stability of particles caused by Nb addition has become an important factor in deteriorating the impact toughness.

V usually exists in the form of VC or VN in steel. V can also exist as a solid solution, but only when the amount of C in the matrix is less. V does not readily precipitate in austenite because of the low dissolution temperature of vanadium nitrides or carbides. Therefore, during welding, the prominent character of V is the promotion of IAF nucleation during the transformation of austenite to ferrite. VN or V(C,N) has a good coherent crystallographic relationship with ferrites and is effective in promoting the nucleation of polygonal and acicular ferrites [41]. According to Wang *et al.* [139], the complex precipitation of V on Ti–Mg–Ce oxide promotes the ferrite-nucleating ability in the HAZ of Ti–Mg–Ce–V deoxidation steels after HHIW. Bian *et al.* [126] studied the influence of Mg deoxidation and V content on the HAZ of EH36 steel and revealed that the impact toughness of HAZ after HHIW can be further improved by Mg deoxidation at high V contents. Mg and V additions refine the size of the precipitates and increase the volume fraction of IAF in the HAZ because the precipitations of (V,Ti)N–MnS inclusions are effective particles for IAF nucleation that combine the low-interface energy and Mn-poor zone mechanisms.

4.3. Effects of Cr, Mo, and B

Alloying elements, such as Cr and Mo, are usually added to enhance the hardenability to achieve high tensile strength for HSLA steels. However, this process inevitably increases the brittle microstructures, such as M–A constituent, which have an adverse impact on the welding performance.

Cr is a strong carbide-forming element commonly used to improve steel hardenability. Cr dissolves into Fe matrix,

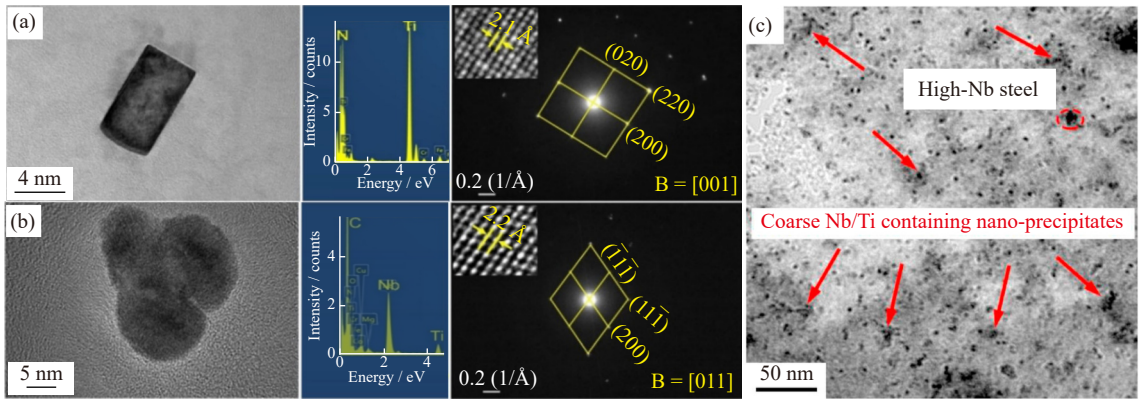

Fig. 13. Effect of Nb addition on precipitates in CGHAZ: morphologies, energy dispersive X-ray spectroscopy, and selected area diffraction pattern analyses for particles in (a) low-Nb and (b) high-Nb steels; (c) micrographs of precipitates in high-Nb steel. (a, b) Reprinted by permission from Springer Nature: *Metall. Mater. Trans. A,* Microstructure evolution in heat-affected zone of shipbuilding steel plates with Mg deoxidation containing different Nb contents, X.Q. Pan, J. Yang, and Y.H. Zhang, Copyright 2022 [136]. (c) Reprinted from *J. Mater. Res. Technol.*, 18, Y.L. Yang, X. Jia, Y.X. Ma, *et al.*, Effect of Nb on microstructure and mechanical properties between base metal and high heat input coarse-grain HAZ in a Ti-deoxidized low carbon high strength steel, 2399-2412, Copyright 2022, with permission from Elsevier [138].

shrinks the austenite phase region, and promotes ferrite transformation [140–141]. Therefore, Cr addition in steels profoundly improves the strength and hardness. A study on the effect of Cr content on the microstructure and mechanical properties of weld metals for HSLA steel showed that Cr can suppress the formation of pearlite and GBF, thus promoting IAF formation [142]. However, the increase in Cr content also leads to an increase in the volume fraction of M–A constituents and a decrease in the impact toughness [143]. Huang *et al.* [144] studied the effect of Cr content on the microstructure and impact toughness in the simulated CGHAZ of HSLA steel and showed that with the increasing Cr content from 0.33wt% to 0.65wt% and 1.02 wt%, the fraction of IAF decreases and that of M–A constituent increases, thus impairing HAZ toughness. To the authors' knowledge, the data on the effect of Cr content on microstructure and impact toughness in the simulated CGHAZ of HSLA steels after HHIW are quite limited, especially for steels using oxide metallurgy.

Mo is also a common alloying element added in high-strength steels for improved hardenability. Wang *et al.* [62] demonstrated that Mo addition for HHIW shipbuilding steel can shrink the austenitic phase zone, effectively induce IAF, promote the transformation of ferrite, and inhibit the transformation of proeutectoid ferrite, thereby improving HAZ toughness. According to Wu *et al.* [145], Mo addition can increase the number density and decrease the size of precipitates by inducing a decrease in lattice parameter. The complex precipitates containing Mo seem to present good thermal stability. Hua *et al.* [146] found that, in thermodynamics, the segregation of Mo toward the austenite/TiC interface releases interfacial energy and induces phase transformation from austenite to ferrite on the precipitated TiC particles. In kinetics, the Mo solute can effectively suppress the diffusion of C atoms. Our previous works reported the effect of Mo content on the impact toughness of HAZ in offshore engineering steel with Ca deoxidation after HHIW [58,134]. The results show that with the increasing Mo content, the toughness at −40°C increases, as pictured in Fig. 14(a). As presented in Fig. 14(b)–(f), the precipitation of TiN and MoC particles and the stability of TiN particles in high-Mo steel increase with the increasing Mo addition. During the thermal cycle, the particle volume fractions and particle pinning forces in low-Mo steel are both smaller than those in high-Mo steel. As a consequence, the PAG size decreases with the increasing Mo content, leading to an increase in LB and a decrease in GB and IAF in CGHAZ. Therefore, Mo addition can promote IAF nucleation and improve the high-temperature stability of precipitates.

B is known as the effective element that can be used instead of C and other alloying elements to bolster steel strength. A small amount of B addition with the order of ppm can significantly affect the microstructure and mechanical properties [147]. The segregation of B atoms at the PAG boundary lowers the grain boundary energy and thus suppresses ferrite nucleation at the PAG boundary [148]. Yamamo *et al.* [79] found that the B segregated at the Ti_2O_3/austenite interface is absorbed into cation vacancies in Ti_2O_3, and the B-depleted zone is formed to promote IAF transformation, as presented in Fig. 5(a). According to our previous studies, B addition significantly increases the toughness in HAZ after HHIW of 400 kJ·cm^{-1} for Mg- or Ca-deoxidized shipbuilding steel plates [147,149]. Fig. 15(a) shows that with the increasing B content, the size and amount of GBFs and FSPs are reduced in CGHAZ microstructures, which are dominated by the refined IAFs. B is segregated on the PAG boundaries and present in the precipitates as presented in Fig. 15(b)–(d). B segregation decreases the boundary energy and delays Mn diffusion to the PAGs, which suppresses the nucleation density of GBFs and FSPs so that IAF formation is increased. However, Funakoshi *et al.* [14] investigated the effects of B addition on the toughness in the weld bond of HSLA with REM deoxidation after HHIW. When the total B (T.B) content is small, the boron nitride content increases with the B content, promoting the forma-

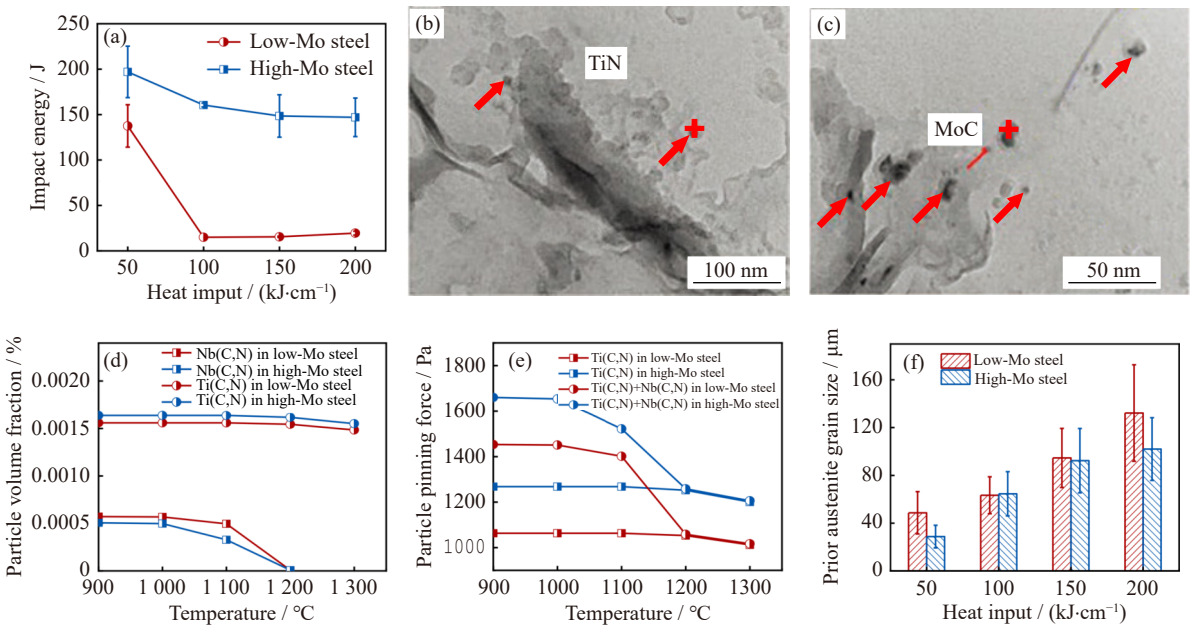

Fig. 14. Effect of Mo addition on the HAZ: (a) change in −40°C Charpy impact toughness of HAZs for the steels with different Mo contents; transmission electron microscope photographs of nanoscale particle in (b) low-Mo and (c) high-Mo steels; (d) calculated volume fractions of Ti(C,N) and Nb(C,N); (e) pinning forces of Ti(C,N) + Nb(C,N) and Ti(C,N) particles; (f) comparison of average PAG sizes in two steels. (a, d–f) Reprinted by permission from Springer Nature: *J. Iron Steel Res. Int.*, Effect of Mo content on nano-scaled particles, prior austenite grains and impact toughness of CGHAZ in offshore engineering steels, D.K. Liu, J. Yang, Y.H. Zhang, and L.Y. Xu, Copyright 2022 [134]. (b, c) Reprinted with permission from Ref. [58]. © 2022 The Iron and Steel Institute of Japan.

tion of fine ferrite grains at the weld bond and improving the toughness. However, the B content becomes saturated as the T.B content approaches 30 ppm, above which the amount of B as Fe–boron carbide abruptly increases, accelerating the nucleation of ferrite on the PAG boundary. Therefore, the B segregation at the grain boundaries and the B-depleted zone around inclusions are crucial for improving the impact toughness.

4.4. Effect of C_{eq}

The C_{eq} is calculated by adding the effects of the other alloying elements to the effect of carbon, which helps assess the weldability of a material. The C_{eq} of high-strength steel is usually greater than 0.4wt%. The reports on the effect of C_{eq} on the mechanical properties and microstructures in the HAZ of the steels with strong deoxidizer addition are quite limited. For steels with high yield strength, Cr, Mo, and V microalloying elements are usually employed with the increased C_{eq} [18]. For steels with high contents of alloying elements, UB and GB are easily formed under a low cooling rate. Therefore, inducing IAF nucleation is more difficult in steel with high C_{eq} than in ferrite steel [2]. Owing to the high content of varied alloying elements in this type of steel, the kinds of carbides or nitrides in the steel are also complex. Therefore, the behavior of these carbides during welding, such as coarsening, dissolution, and reprecipitation, directly affects the growth of austenite grains at high temperatures and the mechanical properties of the HAZ after cooling.

For steel with high C_{eq}, a high toughness can be obtained when the BF or martensite microstructures are refined and the alloy carbides or nitrides in the steel matrix are dispersed [2,29] According to Geng *et al.* [2], Ce addition can improve the toughness of the base metal and CGHAZ of 800-MPa HSLA steel (C_{eq} is about 0.5wt% according to the standard of the international institute of welding) by refining the martensite/bainite blocks and austenite grains. Although the addition of Ce does not induce the IAF formation, the refined martensite/bainite blocks still increase the content of HAGBs, which increasing the crack propagation energy. However, our previous works discovered that with the increasing Mg content from 0.0002wt% to 0.0042wt%, the average impact energy of the HAZ of the offshore engineering steels (C_{eq} is about 0.53 according to the standard of the international institute of welding) at −40°C decreases dramatically [18,39]. On the one hand, the particles in the high-Mg steel dissolve easily and the PAG grows faster, leading to the coarsening bainitic laths. On the other hand, increasing the cementite content, which contains of C, Ni, Cr, and Mn, further increases the LAGBs and reduces impact toughness. Therefore, for steel with high C_{eq}, HAZ toughness can be improved by avoiding the coarsening of austenite grain and refining the microstructures in HAZ, but not by inducing IAF formation.

5. Discussions and prospects

Although oxide metallurgy technology has been utilized for the steel plates of shipbuilding steel, marine steel, and pipeline steel, its large-scale applications are still under development. Numerous technical issues still require further

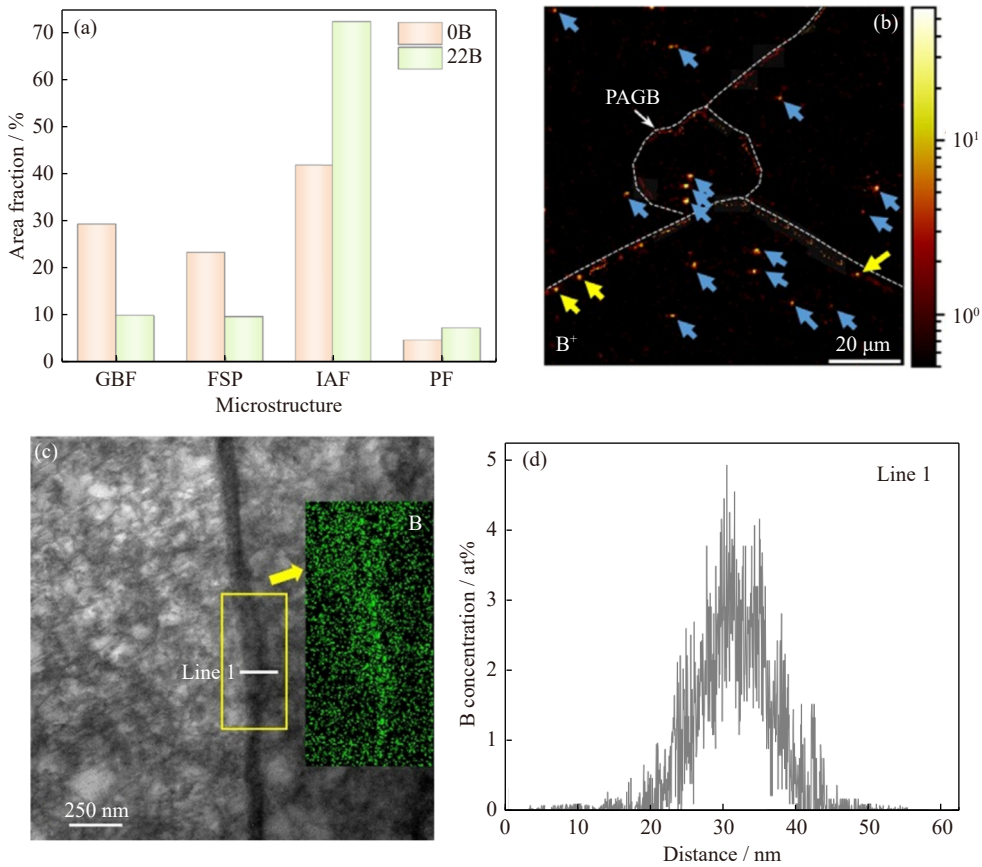

Fig. 15. Effect of B addition on the CGHAZ: (a) area fractions of different microstructures; (b) B^+ mapping results in CGHAZ microstructures of steel with 0.0022wt% B revealed by the time-of-flight secondary-ion mass spectrometry (points with high B^+ around the grain boundary are signed by the yellow arrows, and those in the grain are signed by the blue arrows); (c) magnified views of PAGBs with the EDS mapping results; (d) B concentration profile across the PAGB along line 1 in (c). X.Q. Pan, J. Yang, and Y.H. Zhang, *Steel Res. Int.*, vol. 93, art. No. 2200102 (2022) [147]. Copyright Wiley-VCH Verlag GmbH. Reproduced with permission.

study. An example is the difficulty in controlling the size of inclusions in steelmaking within the preferential size range to induce IAF nucleation and avoid their harmful impact on the mechanical properties of steel plates. In addition, high requirements for the purity of molten steel and continuous casting are needed to obtain fine dispersed inclusions in the molten steel. However, the use of endogenous inclusions to induce acicular ferrite is still the mainstream of oxide metallurgy technology. Hitherto, most studies focused on inclusions formed either during deoxidation or solidification.

Strong deoxidizers such as Ca, Mg, and Zr are usually added together with Ti to achieve the dispersed distribution of fine-sized oxides. Most inclusions serving as active inclusions for IAF nucleation are complex and multiphase. However, some problems remain to be addressed, such as the accurate control of the content of Ti, Ca, Mg, and Zr and the clustering and growing of the high-melting-point inclusions. In addition, some inclusions cause divisions in the potency of inducing IAF nucleation. Nonmetallic inclusions found in steels usually consist of a mixture of several crystalline and/or amorphous phases, so identifying the specific phase responsible for IAF nucleation becomes inherently difficult. Therefore, the first principle calculation method has great potential to prove the nucleation effect of particles.

Combinations of two or three microalloying elements are normally adopted to improve the strength, plasticity, and toughness of steels. The influence of alloying elements on the HAZ of HSLA steel usually includes several aspects. First is to enhance the formation of IAF by providing effective nucleation sites or bainite transformation, second is to promote the precipitation of carbides at low temperatures, and third is to modify the nitrides of Ti. The interactions between various alloy elements are relatively complex, resulting in the generation of complex precipitates whose compositions and formation sequences are important for the mechanical properties of the welding HAZ of steels. For example, the effect of Nb content in Ti-bearing steel is complex. For base metal, Nb addition promotes efficient precipitation hardening through the formation of NbC or Nb(C,N). However, due to the instability of NbC and Nb(C,N) under high temperatures, the pinning effect of precipitation significantly increases [86,136–137]. The addition of microalloying elements is also beneficial to improving the hardenability and increasing the content of brittle microstructures. Moreover, microalloying elements may exhibit different effects on oxide metallurgy technology. For example, when Mg and V compounds are added simultaneously, the interaction between Mg-induced inclusions and V-induced particles complicates the formation of the secondary phase particles [106,139]. Therefore, in-depth research is needed to study the mechanism of how

microalloying elements work and interact with each other in the HAZ of HSLA steel after HHIW.

6. Conclusions

In this study, the fundament and industrial application of oxide metallurgy and the effects of deoxidation methods and microalloying elements on oxide metallurgy technology are discussed to elucidate the progress of oxide metallurgy technology in improving the weldability of HSLA steel. The following conclusions are drawn.

(1) Oxide metallurgy integrates two factors: (i) inducing IAF using specific inclusions and precipitates to refine the microstructures and (ii) restricting the growth of PAGs by nanosized particles during the welding of steel. So far, the typical oxide metallurgy technologies with successful industrial applications include HTUFF, JFE EWEL, KST, and ET-ISD.

(2) The complex deoxidation of Ti with other strong deoxidant elements such as Mg, Ca, Zr, and REMs can improve HAZ toughness. Mg addition can refine the Ti_2O_3 inclusions. The strong affinity of Mg with oxygen is beneficial for the precipitation of fine and dispersed TiN particles. In Ca-treated steel, Ca-oxysulfide easily forms and is beneficial for reducing individual MnS precipitates and promoting IAF nucleation. In REM- and Zr-treated steels, the superior impact toughness is attributed to the high fraction of IAF and the low fraction of the M–A constituent, respectively.

(3) Increasing the C, Si, Al, Nb, and Cr contents impairs HAZ toughness. A high C content usually increases the number of coarse carbides and decreases the potency of IAF formation. Increasing the Si content causes the coarsening of the microstructures. Si and Cr addition can increase the contents of brittle microstructures, such as the M–A constituent. The high Al content in steel is not beneficial for IAF nucleation due to the formation of Al_2O_3 inclusions. Nb is soluble in TiN particles to form (Ti,Nb)(C,N) particles, which have poor high-temperature stability. Mo, V, and B can enhance HAZ toughness. Mo-containing precipitates present good thermal stability. Hence, an appropriate increase in Mo content can refine precipitates and promote the transformation of IAF. VN or V(C,N) is effective in promoting IAF nucleation due to its good coherent crystallographic relationship with ferrite. The segregation of B atoms at the PAG boundary and the B-depleted zone around the inclusion suppress the ferrite nucleation at the PAG boundary and promote IAF formation.

Acknowledgements

This work is financially supported by the National Natural Science Foundation of China (No. U1960202).

Conflict of Interest

Jian Yang is an editorial board member for this journal and was not involved in the editorial review or the decision to publish this article. On behalf of all of the authors, the corresponding author states that there is no conflict of interest.

References

[1] Y.H. Zhang, J. Yang, H.L. Du, Y. Zhang, and H. Ma, Effect of Ca deoxidation on toughening of heat-affected zone in high-strength low-alloy steels after large-heat-input welding, *Metals*, 12(2022), No. 11, p. 1830.

[2] R.M. Geng, J. Li, C.B. Shi, J.G. Zhi, and B. Lu, Effect of Ce on microstructures, carbides and mechanical properties in simulated coarse-grained heat-affected zone of 800-MPa high-strength low-alloy steel, *Mater. Sci. Eng. A*, 840(2022), art. No. 142919.

[3] M.J. Zhao, L.H. Jiang, C.M. Li, L. Huang, C.Y. Sun, J.J. Li, and Z.H. Guo, Flow characteristics and hot workability of a typical low-alloy high-strength steel during multi-pass deformation, *Int. J. Miner. Metall. Mater.*, 31(2024), No. 2, p. 323.

[4] J. Kang, C.N. Li, X.L. Li, J.H. Zhao, G. Yuan, and G.D. Wang, Effects of processing variables on microstructure and yield ratio of high strength constructional steels, *J. Iron Steel Res. Int.*, 23(2016), No. 8, p. 815.

[5] P. Han, Z.P. Liu, Z.J. Xie, *et al*., Influence of band microstructure on carbide precipitation behavior and toughness of 1 GPa-grade ultra-heavy gauge low-alloy steel, *Int. J. Miner. Metall. Mater.*, 30(2023), No. 7, p. 1329.

[6] M.H. Liu, Z.Y. Liu, C.W. Du, *et al*., Effect of cathodic potential on stress corrosion cracking behavior of 21Cr_2NiMo steel in simulated seawater, *Int. J. Miner. Metall. Mater.*, 29(2022), No. 2, p. 263.

[7] E.D. Fan, S.Q. Zhang, D.H. Xie, Q.Y. Zhao, X.G. Li, and Y.H. Huang, Effect of nanosized NbC precipitates on hydrogen-induced cracking of high-strength low-alloy steel, *Int. J. Miner. Metall. Mater.*, 28(2021), No. 2, p. 249.

[8] E.D. Fan, Y. Li, Y. You, and X.W. Lü, Effect of crystallographic orientation on crack growth behaviour of HSLA steel, *Int. J. Miner. Metall. Mater.*, 29(2022), No. 8, p. 1532.

[9] D.P. Zhu, W. Zhang, Z.X. Ding, and J. Kim, Investigation of crack propagation driving force based on crystal plasticity and cyclic J-integral, *Eng. Fract. Mech.*, 289(2023), art. No. 109362.

[10] Y.D. Wang, Z.H. Tang, S.F. Xiao, C. WSiyasiya, and T. Wei, Effects of final rolling temperature and coiling temperature on precipitates and microstructure of high-strength low-alloy pipeline steel, *J. Iron Steel Res. Int.*, 29(2022), No. 8, p. 1236.

[11] Y. Liu, G.Q. Li, X.L. Wan, X.G. Zhang, Y. Shen, and K.M. Wu, Toughness improvement by Zr addition in the simulated coarse-grained heat-affected zone of high-strength low-alloy steels, *Ironmaking Steelmaking*, 46(2019), No. 2, p. 113.

[12] W.L. Wang, L.K. Wang, and P.S. Lyu, Kinetics of austenite growth and bainite transformation during reheating and cooling treatments of high strength microalloyed steel produced by sub-rapid solidification, *Int. J. Miner. Metall. Mater.*, 30(2023), No. 2, p. 354.

[13] X. Wang, C. Wang, J. Kang, G. Yuan, R.D.K. Misra, and G.D. Wang, Improved toughness of double-pass welding heat affected zone by fine Ti–Ca oxide inclusions for high-strength low-alloy steel, *Mater. Sci. Eng. A*, 780(2020), art. No. 139198.

[14] T. Funakoshi, T. Tanaka, S. Ueda, M. Ishikawa, N. Koshizuka, and K. Kobayashi, Improvement in microstructure and toughness of large heat-input weld bond of high strength steel due to addition of rare earth metals and boron, *ISIJ Int.*, 17(1977), No. 7, p. 419.

[15] H.N. Lou, C. Wang, B.X. Wang, Z.D. Wang, and R.D.K.

Misra, Effect of Ti–Mg–Ca treatment on properties of heat-affected zone after high heat input welding, *J. Iron Steel Res. Int.*, 26(2019), No. 5, p. 501.
[16] J. Yang, K. Zhu, R.Z. Wang, and J.G. Shen, Improving the toughness of heat affected zone of steel plate by use of fine inclusion particles, *Steel Res. Int.*, 82(2011), No. 5, p. 552.
[17] C. Ouchi, Development of steel plates by intensive use of TMCP and direct quenching processes, *ISIJ Int.*, 41(2001), No. 6, p. 542.
[18] X.Q. Pan, J.J. Zhi, Z.J. Fan, Y.H. Zhang, and J. Yang, Relationship between the microstructure and impact toughness of the coarse-grained heat-affected zone for offshore engineering steels with different Mg contents, *Steel Res. Int.*, 92(2021), No. 10, art. No. 2100099.
[19] M.H. Shi, P.Y. Zhang, C. Wang, and F.X. Zhu, Effect of high heat input on toughness and microstructure of coarse grain heat affected zone in Zr bearing low carbon steel, *ISIJ Int.*, 54(2014), No. 4, p. 932.
[20] B.W. Zhou, G.Q. Li, X.L. Wan, Y. Li, and K.M. Wu, *In-situ* observation of grain refinement in the simulated heat-affected zone of high-strength low-alloy steel by Zr–Ti combined deoxidation, *Met. Mater. Int.*, 22(2016), No. 2, p. 267.
[21] A.M. Guo, S.R. Li, J. Guo, *et al*., Effect of zirconium addition on the impact toughness of the heat affected zone in a high strength low alloy pipeline steel, *Mater. Charact.*, 59(2008), No. 2, p. 134.
[22] Y. Shen, X.L. Wan, Y. Liu, G.Q. Li, Z.L. Xue, and K.M. Wu, The significant impact of Ti content on microstructure–toughness relationship in the simulated coarse-grained heated-affected zone of high-strength low-alloy steels, *Ironmaking Steelmaking*, 46(2019), No. 6, p. 584.
[23] W.Z. Mu, P.G. Jönsson, and K. Nakajima, Recent aspects on the effect of inclusion characteristics on the intragranular ferrite formation in low alloy steels: A review, *High Temp. Mater. Process.*, 36(2017), No. 4, p. 309.
[24] D.S. Sarma, A.V. Karasev, and P.G. Jönsson, On the role of non-metallic inclusions in the nucleation of acicular ferrite in steels, *ISIJ Int.*, 49(2009), No. 7, p. 1063.
[25] S.S. Babu, The mechanism of acicular ferrite in weld deposits, *Curr. Opin. Solid State Mater. Sci.*, 8(2004), No. 3-4, p. 267.
[26] T. Koseki, and G. Thewlis, Overview inclusion assisted microstructure control in C–Mn and low alloy steel welds, *Mater. Sci. Technol.*, 21(2005), No. 8, P. 867.
[27] Y. Shao, C.X. Liu, Z.S. Yan, H.J. Li, and Y.C. Liu, Formation mechanism and control methods of acicular ferrite in HSLA steels: A review, *J. Mater. Sci. Technol.*, 34(2018), No. 5, p. 737.
[28] Z.T. Ma, D. Peisker, and D. Janke, Grain refining of structural steels by dispersion of fine oxide particles, *Steel Res.*, 70(1999), No. 4-5, p. 178.
[29] W. Liang, R.M. Geng, J.G. Zhi, J. Li, and F. Huang, Oxide metallurgy technology in high strength steel: A review, *Materials*, 15(2022), No. 4, art. No. 1350.
[30] F. Pan, J. Zhang, H.L. Chen, *et al*., Effects of rare earth metals on steel microstructures, *Materials*, 9(2016), No. 6, art. No. E417.
[31] J. Yang, K. Zhu, and G.D. Wang, Progress in the technological development of oxide metallurgy for manufacturing steel plates with excellent HAZ toughness, *Baosteel Tech. Res.*, 2(2008), No. 4, p. 43.
[32] X.Q. Pan, J. Yang, Y.H. Zhang, and R.B. Li, Effect of Si content on the microstructures and toughness in heat-affected zone of offshore engineering steels with Mg deoxidation, *Steel Res. Int.*, 94(2023), No. 3, art. No. 2200534.
[33] Z.F. Wang, M.H. Shi, S. Tang, and G.D. Wang, Effect of heat input and M–A constituent on microstructure evolution and mechanical properties of heat affected zone in low carbon steel, *J. Wuhan Univ. Technol. Mater. Sci. Ed.*, 32(2017), No. 5, p. 1163.
[34] Y.K. Yang, D.P. Zhan, H. Lei, *et al*., Coupling effect of prior austenite grain size and inclusion characteristics on acicular ferrite formation in Ti–Zr deoxidized low carbon steel, *Metall. Mater. Trans. B*, 51(2020), No. 2, p. 480.
[35] X.J. Liu, G. Yuan, R.D.K. Misra, and G.D. Wang, A comparative study of acicular ferrite transformation behavior between surface and interior in a low C–Mn steel by HT-LSCM, *Metals*, 11(2021), No. 5, art. No. 699.
[36] B. Hwang, C.G. Lee, and T.H. Lee, Correlation of microstructure and mechanical properties of thermomechanically processed low-carbon steels containing boron and copper, *Metall. Mater. Trans. A*, 41(2010), No. 1, p. 85.
[37] L.Y. Xu, J. Yang, R.Z. Wang, Y.N. Wang, and W.L. Wang, Effect of Mg content on the microstructure and toughness of heat-affected zone of steel plate after high heat input welding, *Metall. Mater. Trans. A*, 47(2016), No. 7, p. 3354.
[38] X. Wang, C. Wang, J. Kang, G.D. Wang, D. Misra, and G. Yuan, Relationship between impact toughness and microstructure for the as-rolled and simulated HAZ of low-carbon steel containing Ti–Ca oxide particles, *Metall. Mater. Trans. A*, 51(2020), No. 6, p. 2927.
[39] X.Q. Pan, J.J. Zhi, Z.J. Fan, Y.H. Zhang, R.B. Li, and J. Yang, Morphology and crystallography of microstructures in Mg-deoxidized offshore engineering steels after simulated welding thermal cycles, *Ironmaking Steelmaking*, 49(2022), No. 5, p. 541.
[40] Y.S. Yu, B. Hu, M.L. Gao, *et al*., Determining role of heterogeneous microstructure in lowering yield ratio and enhancing impact toughness in high-strength low-alloy steel, *Int. J. Miner. Metall. Mater.*, 28(2021), No. 5, p. 816.
[41] T. Furuhara, T. Shinyoshi, G. Miyamoto, *et al*., Multiphase crystallography in the nucleation of intragranular ferrite on MnS+V(C,N) complex precipitate in austenite, *ISIJ Int.*, 43(2003), No. 12, p. 2028.
[42] R.A. Ricks, P.R. Howell, and G.S. Barritte, The nature of acicular ferrite in HSLA steel weld metals, *J. Mater. Sci.*, 17(1982), No. 3, p. 732.
[43] H.H. Jin, J.H. Shim, Y.W. Cho, and H.C. Lee, Formation of intragranular acicular ferrite grains in a Ti-containing low carbon steel, *ISIJ Int.*, 43(2003), No. 7, p. 1111.
[44] H. Mabuchi, R. Uemori, and M. Fujioka, The role of Mn depletion in intra-granular ferrite transformation in the heat affected zone of welded joints with large heat input in structural steels, *ISIJ Int.*, 36(1996), No. 11, p. 1406.
[45] J.S. Byun, J.H. Shim, Y.W. Cho, and D.N. Lee, Non-metallic inclusion and intragranular nucleation of ferrite in Ti-killed C–Mn steel, *Acta Mater.*, 51(2003), No. 6, p. 1593.
[46] G. Thewlis, J.A. Whiteman, and D.J. Senogles, Dynamics of austenite to ferrite phase transformation in ferrous weld metals, *Mater. Sci. Technol.*, 13(1997), No. 3, p. 257.
[47] X. Wang, C. Wang, J. Kang, G. Yuan, R.D.K. Misra, and G.D. Wang, An *in situ* microscopy study on nucleation and growth of acicular ferrite in Ti–Ca–Zr deoxidized low-carbon steel, *Mater. Charact.*, 165(2020), art. No. 110381.
[48] Y. Terazawa, K. Ichimiya, and K. Hase, Nucleation effect of Ca-oxysulfide inclusions of low carbon steel in heat affected zone by welding, *Mater. Sci. Forum*, 941(2018), p. 130.
[49] L.Y. Xu, J. Yang, R.Z. Wang, W.L. Wang, and Y.N. Wang, Effect of Mg addition on formation of intragranular acicular ferrite in heat-affected zone of steel plate after high-heat-input welding, *J. Iron Steel Res. Int.*, 25(2018), No. 4, p. 433.
[50] L.Y. Xu, J. Yang, and R.Z. Wang, Influence of Al content on the inclusion-microstructure relationship in the heat-affected zone of a steel plate with Mg deoxidation after high-heat-input welding, *Metals*, 8(2018), No. 12, art. No. 1027.

[51] S. St-Laurent and G. L'Espérance, Effects of chemistry, density and size distribution of inclusions on the nucleation of acicular ferrite of C–Mn steel shielded-metal-arc-welding weldments, *Mater. Sci. Eng. A*, 149(1992), No. 2, p. 203.
[52] Z.H. Wu, W. Zheng, G.Q. Li, H. Matsuura, and F. Tsukihashi, Effect of inclusions' behavior on the microstructure in Al–Ti deoxidized and magnesium-treated steel with different aluminum contents, *Metall. Mater. Trans. B*, 46(2015), No. 3, p. 1226.
[53] J.L. Lee and Y.T. Pan, Effect of sulfur content on the microstructure and toughness of simulated heat-affected zone in Ti-killed steels, *Metall. Trans. A*, 24(1993), No. 6, p. 1399.
[54] X.S. Tian, L.F. Zhu, Z.Y. Cai, and H. Kong, The relationship between MnS precipitation and induced nucleation effect of Mg-bearing inclusion, *High Temp. Mater. Process.*, 37(2018), No. 8, p. 711.
[55] X.Z. Gao, S.F. Yang, J.S. Li, H. Liao, W. Gao, and T. Wu, Addition of MgO nanoparticles to carbon structural steel and the effect on inclusion characteristics and microstructure, *Metall. Mater. Trans. B*, 47(2016), No. 2, p. 1124.
[56] F.J. Barbaro, P. Krauklis, and K.E. Easterling, Formation of acicular ferrite at oxide particles in steels, *Mater. Sci. Technol.*, 5(1989), No. 11, p. 1057.
[57] B. Kim, S. Uhm, C. Lee, J. Lee, and Y. An, Effects of inclusions and microstructures on impact energy of high heat-input submerged-arc-weld metals, *J. Eng. Mater. Technol.*, 127(2005), No. 2, p. 204.
[58] D.K. Liu, J. Yang, and Y.H. Zhang, *In-situ* observation of bainite transformation in CGHAZ of 420 MPa grade offshore engineering steel with different Mo contents, *ISIJ Int.*, 62(2022), No. 4, p. 714.
[59] H. Suito, A.V. Karasev, M. Hamada, R. Inoue, and K. Nakajima, Influence of oxide particles and residual elements on microstructure and toughness in the heat-affected zone of low-carbon steel deoxidized with Ti and Zr, *ISIJ Int.*, 51(2011), No. 7, p. 1151.
[60] S. Kanazawa, A. Nakashima, K. Okamoto, and K. Kanaya, Improved toughness of weld fussion zone by fine TiN particles and development of a steel for large heat input welding, *Tetsu-to-Hagane*, 61(1975), No. 11, p. 2589.
[61] J. Takamura and S. Mizoguchi, Roles of oxides in steels performance, [in] *Proceedings of the 6th International Iron and Steel Congress*, Japan, 1990, p. 591.
[62] Y. Wang, L.G. Zhu, Q.J. Zhang, C.J. Zhang, and S.M. Wang, Effect of Mg treatment on refining the microstructure and improving the toughness of the heat-affected zone in shipbuilding steel, *Metals*, 8(2018), No. 8, art. No. 616.
[63] J. Yang, L.Y. Xu, K. Zhu, R.Z. Wang, L.J. Zhou, and W.L. Wang, Improvement of HAZ toughness of steel plate for high heat input welding by inclusion control with Mg deoxidation, *Steel Res. Int.*, 86(2015), No. 6, p. 619.
[64] X.D. Zou, D.P. Zhao, J.C. Sun, C. Wang, and H. Matsuura, An integrated study on the evolution of inclusions in EH36 shipbuilding steel with Mg addition: From casting to welding, *Metall. Mater. Trans. B*, 49(2018), No. 2, p. 481.
[65] A. Kojima, A. Kiyose, R. Uemori, *et al*., Super high HAZ toughness technology with fine microstructure imparted by fine particles, *Nippon Steel Tech. Rep.*, 90(2004), p. 2.
[66] T. Kimura, H. Sumi, and Y. Kitani, High tensile strength steel plates and welding consumables for architectural construction with excellent toughness in welded joint – "JFE EWEL" technology for excellent quality in HAZ of high heat input welded joints, *JFE Tech. Rep*., (2005), No. 5, p. 45.
[67] T. Kato, S. Sato, H. Ohta, and T. Shiwaku, Effects of Ca addition on formation behavior of TiN particles and HAZ toughness in large heat input welding, *Kobelco Technol. Rev.*, 30(2011), p. 76.
[68] Y. Jian, Z. Kai, W.R. Zhi, and S.J. Guo, Excellent heat affected zone toughness technology improved by use of strong deoxidizers, *J. Iron Steel Res. Int.*, 18(2011), No. S2, p. 141.
[69] J.H. Shim, Y.J. Oh, J.Y. Suh, *et al*., Ferrite nucleation potency of non-metallic inclusions in medium carbon steels, *Acta Mater.*, 49(2001), No. 12, p. 2115.
[70] J.S. Byun, J.H. Shim, J.Y. Suh, *et al*., Inoculated acicular ferrite microstructure and mechanical properties, *Mater. Sci. Eng. A*, 319-321(2001), p. 326.
[71] K. Hui, S. Shao, Y.F. Shen, *et al*., Effect of aluminum on the nucleation of intragranular ferrite in Ti-added carbon structural steel, *High Temp. Mater. Process.*, 32(2013), No. 3, p. 323.
[72] S.Z. Wang, Z.J. Gao, G.L. Wu, and X.P. Mao, Titanium microalloying of steel: A review of its effects on processing, microstructure and mechanical properties, *Int. J. Miner. Metall. Mater.*, 29(2022), No. 4, p. 645.
[73] F. Chai, C.F. Yang, H. Su, Y.Q. Zhang, and D.D. Zhang, Effect of aluminum and titanium treatment on non-metallic inclusions and microstructures of CGHAZ in HSLA steel, *J. Iron Steel Res. Int.*, 18(2011), No. S1, p. 360.
[74] C.J. Xuan, W.Z. Mu, Z.I. Olano, P.G. Jönsson, and K. Nakajima, Effect of the Ti, Al contents on the inclusion characteristics in steels with TiO_2 and TiN particle additions, *Steel Res. Int.*, 87(2016), No. 7, p. 911.
[75] Z.H. Xiong, S.L. Liu, X.M. Wang, C.J. Shang, and R.D.K. Misra, Relationship between crystallographic structure of the Ti_2O_3/MnS complex inclusion and microstructure in the heat-affected zone (HAZ) in steel processed by oxide metallurgy route and impact toughness, *Mater. Charact.*, 106(2015), p. 232.
[76] K. Seo, Y.M. Kim, G.M. Evans, H.J. Kim, and C. Lee, Formation of Mn-depleted zone in Ti-containing weld metals, *Weld. World*, 59(2015), No. 3, p. 373.
[77] F. Chai, H. Su, C.F. Yang, and D.M. Xue, Nucleation behavior analysis of intragranular acicular ferrite in a Ti-killed C–Mn steel, *J. Iron Steel Res. Int.*, 21(2014), No. 3, p. 369.
[78] T. Yamada, H. Terasaki, and Y.I. Komizo, Relation between inclusion surface and acicular ferrite in low carbon low alloy steel weld, *ISIJ Int.*, 49(2009), No. 7, p. 1059.
[79] K. Yamamoto, T. Hasegawa, and J.I. Takamura, Effect of boron on intra-granular ferrite formation in Ti-oxide bearing steels, *ISIJ Int.*, 36(1996), No. 1, p. 80.
[80] A.R. Mills, G. Thewlis, and J.A. Whiteman, Nature of inclusions in steel weld metals and their influence on formation of acicular ferrite, *Mater. Sci. Technol.*, 3(1987), No. 12, p. 1051.
[81] J.H. Shim, J.S. Byun, Y.W. Cho, Y.J. Oh, J.D. Shim, and D.N. Lee, Mn absorption characteristics of Ti_2O_3 inclusions in low carbon steels, *Scripta Mater.*, 44(2001), No. 1, p. 49.
[82] J.H. Shim, Y.W. Cho, S.H. Chung, J.D. Shim, and D.N. Lee, Nucleation of intragranular ferrite at Ti_2O_3 particle in low carbon steel, *Acta Mater.*, 47(1999), No. 9, p. 2751.
[83] M. Jiang, X.H. Wang, Z.Y. Hu, K.P. Wang, C.W. Yang, and S.R. Li, Microstructure refinement and mechanical properties improvement by developing IAF on inclusions in Ti–Al complex deoxidized HSLA steel, *Mater. Charact.*, 108(2015), p. 58.
[84] S.F. Medina, M. Chapa, P. Valles, A. Quispe, and M.I. Vega, Influence of Ti and N contents on austenite grain control and precipitate size in structural steels, *ISIJ Int.*, 39(1999), No. 9, p. 930.
[85] Z.X. Zhu, J. Han, and H.J. Li, Effect of alloy design on improving toughness for X70 steel during welding, *Mater. Des.*, 88(2015), p. 1326.
[86] I. Rak, V. Gliha, and M. Koçak, Weldability and toughness assessment of Ti-microalloyed offshore steel, *Metall. Mater. Trans. A*, 28(1997), No. 1, p. 199.
[87] Z.X. Zhu, L. Kuzmikova, M. Marimuthu, H.J. Li, and F. Bar-

baro, Role of Ti and N in line pipe steel welds, *Sci. Technol. Weld. Joining*, 18(2013), No. 1, p. 1.

[88] R.Z. Wang, J. Yang, and L.Y. Xu, Improvement of heat-affected zone toughness of steel plates for high heat input welding by inclusion control with Ca deoxidation, *Metals*, 8(2018), No. 11, art. No. 946.

[89] Q.Y. Wang, X.D. Zou, H. Matsuura, and C. Wang, Evolution of inclusions during 1473 K heating process in EH36 shipbuilding steel with Mg addition, *JOM*, 70(2018), No. 4, p. 521.

[90] Z. Liu, B. Song, Z.B. Yang, *et al*., Effect of cerium content on the evolution of inclusions and formation of acicular ferrite in Ti–Mg-killed EH36 steel, *Metals*, 10(2020), No. 7, art. No. 863.

[91] C. Wang, X. Wang, J. Kang, G. Yuan, and G.D. Wang, Microstructure and mechanical properties of hot-rolled low-carbon steel containing Ti–Ca oxide particles: A comparison between base metal and HAZ, *J. Iron Steel Res. Int.*, 27(2020), No. 4, p. 440.

[92] L. Liang, B. Zhang, L.Y. Yan, *et al*., Evolution behaviour of inclusions via oxide metallurgy of NM450 ultrahigh-strength steel, *Mater. Res. Express*, 8(2021), No. 10, art. No. 105602.

[93] S.Y. Shin, K. Oh, K.B. Kang, and S. Lee, Improvement of Charpy impact properties in heat affected zones of API X80 pipeline steels containing complex oxides, *Mater. Sci. Technol.*, 26(2010), No. 9, p. 1049.

[94] L.Y. Xu, J. Yang, J. Park, and H. Ono, Mechanism of improving heat-affected zone toughness of steel plate with Mg deoxidation after high-heat-input welding, *Metals*, 10(2020), No. 2, art. No. 162.

[95] Y. Wang, L.G. Zhu, J.X. Huo, *et al*., Relationship between crystallographic structure of complex inclusions $MgAl_2O_4$/Ti_2O_3/MnS and improved toughness of heat-affected zone in shipbuilding steel, *J. Iron Steel Res. Int.*, 29(2022), No. 8, p. 1277.

[96] L.G. Sun, H.R. Li, L.G. Zhu, Y.S. Liu, and J. Hwang, Research on the evolution mechanism of pinned particles in welding HAZ of Mg treated shipbuilding steel, *Mater. Des.*, 192(2020), art. No. 108670.

[97] X.D. Zou, J.C. Sun, H. Matsuura, and C. Wang, Documenting ferrite nucleation behavior differences in the heat-affected zones of EH36 shipbuilding steels with Mg and Zr additions, *Metall. Mater. Trans. A*, 50(2019), No. 10, p. 4506.

[98] Y. Liu, X.L. Wan, G.Q. Li, Y. Wang, W. Zheng, and Y.H. Hou, Grain refinement in coarse-grained heat-affected zone of Al–Ti–Mg complex deoxidised steel, *Sci. Technol. Weld. Joining*, 24(2019), No. 1, p. 43.

[99] H.N. Lou, C. Wang, B.X. Wang, Z.D. Wang, Y.Q. Li, and Z.G. Chen, Inclusion evolution behavior of Ti–Mg oxide metallurgy steel and its effect on a high heat input welding HAZ, *Metals*, 8(2018), No. 7, art. No. 534.

[100] L.Y. Xu, J. Yang, R.Z. Wang, W.L. Wang, and Z.M. Ren, Effect of welding heat input on microstructure and toughness of heated-affected zone in steel plate with Mg deoxidation, *Steel Res. Int.*, 88(2017), No. 12, art. No. 1700157.

[101] B. Wen, B. Song, N. Pan, Q.Y. Hu, and J.H. Mao, Effect of SiMg alloy on inclusions and microstructures of 16Mn steel, *Ironmaking Steelmaking*, 38(2011), No. 8, p. 577.

[102] F. Chai, C.F. Yang, H. Su, Y.Q. Zhang, and Z. Xu, Effect of magnesium on inclusion formation in Ti-killed steels and microstructural evolution in welding induced coarse-grained heat affected zone, *J. Iron Steel Res. Int.*, 16(2009), No. 1, p. 69.

[103] H. Kong, Y.H. Zhou, H. Lin, *et al*., The mechanism of intragranular acicular ferrite nucleation induced by Mg–Al–O inclusions, *Adv. Mater. Sci. Eng.*, 2015(2015), art. No. 378678.

[104] Y.H. Hou, W. Zheng, Z.H. Wu, *et al*., Study of Mn absorption by complex oxide inclusions in Al–Ti–Mg killed steels, *Acta Mater.*, 118(2016), p. 8.

[105] L.Y. Xu and J. Yang, Effects of Mg content on characteristics of nanoscale TiN particles and toughness of heat-affected zones of steel plates after high-heat-input welding, *Metall. Mater. Trans. A*, 51(2020), No. 9, p. 4540.

[106] L.G. Zhu, Y. Wang, S.M. Wang, Q.J. Zhang, and C.J. Zhang, Research of microalloy elements to induce intragranular acicular ferrite in shipbuilding steel, *Ironmaking Steelmaking*, 46(2019), No. 6, p. 499.

[107] Y.H. Zhang, J. Yang, L.Y. Xu, *et al*., The effect of Ca content on the formation behavior of inclusions in the heat affected zone of thick high-strength low-alloy steel plates after large heat input weldings, *Metals*, 9(2019), No. 12, art. No. 1328.

[108] Z. Liu, B. Song, and J.H. Mao, Effect of Ca on the evolution of inclusions and the formation of acicular ferrite in Ti–Mg killed EH36 steel, *Ironmaking Steelmaking*, 48(2021), No. 9, p. 1115.

[109] X. Wang, Y. Chen, C. Wang, *et al*., Effect of heat input on microstructure and impact toughness of coarse-grained heat-affected zone in Al–Ca and Ti–Ca killed steels, *Steel Res. Int.*, 91(2020), No. 9, art. No. 2000133.

[110] J.L. Lee and Y.T. Pan, The formation of intragranular acicular ferrite in simulated heat-affected zone, *ISIJ Int.*, 35(1995), No. 8, p. 1027.

[111] Y.X. Cao, X.L. Wan, Y.H. Hou, C.R. Niu, Y. Liu, and G.Q. Li, *In situ* observation of grain refinement in the simulated heat-affected zone of Al–Ti–0.05% Ce-deoxidized steel, *Steel Res. Int.*, 90(2019), No. 9, art. No. 1900084.

[112] Y.H. Zhang, J. Yang, D.K. Liu, X.Q. Pan, and L.Y. Xu, Improvement of impact toughness of the welding heat-affected zone in high-strength low-alloy steels through Ca deoxidation, *Metall. Mater. Trans. A*, 52(2021), No. 2, p. 668.

[113] M.H. Shi, X.G. Yuan, H.J. Huang, and S. Zhang, Effect of Zr addition on the microstructure and toughness of coarse-grained heat-affected zone with high-heat input welding thermal cycle in low-carbon steel, *J. Mater. Eng. Perform.*, 26(2017), No. 7, p. 3160.

[114] F.C. Liu, Y. Bi, C. Wang, *et al*., Inclusion characteristics and acicular ferrite formation in the simulated heat-affected zone of Ti–Zr-killed low-carbon steel, *Met. Mater. Int.*, 29(2023), No. 3, p. 715.

[115] H.B. Liu, J. Kang, X.J. Zhao, *et al*., Influence of Ca treatment on particle–microstructure relationship in heat-affected zone of shipbuilding steel with Zr–Ti deoxidation after high-heat-input welding, *J. Iron Steel Res. Int.*, 29(2022), No. 8, p. 1291.

[116] X.D. Zou, J.C. Sun, D.P. Zhao, H. Matsuura, and C. Wang, Effects of Zr addition on evolution behavior of inclusions in EH36 shipbuilding steel: From casting to welding, *J. Iron Steel Res. Int.*, 25(2018), No. 2, p. 164.

[117] Y. Li, X.L. Wan, L. Cheng, and K.M. Wu, First-principles calculation of the interaction of Mn with ZrO_2 and its effect on the formation of ferrite in high-strength low-alloy steels, *Scripta. Mater.*, 75(2014), p. 78.

[118] J.H. Ma, D.P. Zhan, Z.H. Jiang, J.C. He, and J. Yu, Effect of Ti, Zr and Mg addition on the impact toughness of heat affected zone in low carbon steel, *Adv. Mater. Res.*, 146-147(2010), p. 1486.

[119] Y.K. Yang, D.P. Zhan, H. Lei, G.X. Qiu, Z.H. Jiang, and H.S. Zhang, Formation of non-metallic inclusion and acicular ferrite in Ti–Zr deoxidized steel, *ISIJ Int.*, 59(2019), No. 9, p. 1545.

[120] Y.X. Cao, X.L. Wan, F. Zhou, *et al*., Effect of Ce content on microstructure-toughness relationship in the simulated coarse-grained heat-affected zone of high-strength low-alloy steels, *Metals*, 11(2021), No. 12, art. No. 2003.

[121] Y.X. Cao, X.L. Wan, Y.H. Hou, Y. Liu, M.M. Song, and G.Q. Li, Comparative study on the effect of Y content on grain refinement in the simulated coarse-grained heat-affected zone of

X70 pipeline steels, *Micron*, 127(2019), art. No. 102758.
[122] M.M. Song, Y.M. Xie, B. Song, *et al*., The microstructure and property of the heat affected zone in C–Mn steel treated by rare earth, *High Temp. Mater. Process.*, 38(2019), No. 2019, p. 362.
[123] H. Nako, Y. Okazaki, and J.G. Speer, Acicular ferrite formation on Ti–rare earth metal–Zr complex oxides, *ISIJ Int.*, 55(2015), No. 1, p. 250.
[124] G. Thewlis, Effect of cerium sulphide particle dispersions on acicular ferrite microstructure development in steels, *Mater. Sci. Technol.*, 22(2006), No. 2, p. 153.
[125] N. Yan, S.F. Yu, and Y. Chen, *In situ* observation of austenite grain growth and transformation temperature in coarse grain heat affected zone of Ce-alloyed weld metal, *J. Rare Earths*, 35(2017), No. 2, p. 203.
[126] S.Y. Bian, H.M. Zhao, J.J. Wang, *et al*., Effect of alloy element on microstructure and properties of heat-affected zone, *Mater. Sci. Technol.*, 38(2022), p. 1244.
[127] W.Z. Mu, H.H. Mao, P.G. Jönsson, and K. Nakajima, Effect of carbon content on the potency of the intragranular ferrite formation, *Steel Res. Int.*, 87(2016), No. 3, p. 311.
[128] J.M. Gregg and H.K.D.H. Bhadeshia, Solid-state nucleation of acicular ferrite on minerals added to molten steel, *Acta Mater.*, 45(1997), No. 2, p. 739.
[129] S. Kim, Y.R. Im, S. Lee, H.C. Lee, S.J. Kim, and J.H. Hong, Effects of alloying elements on fracture toughness in the transition temperature region of base metals and simulated heat-affected zones of Mn–Mo–Ni low-alloy steels, *Metall. Mater. Trans. A*, 35(2004), No. 7, p. 2027.
[130] D.K. Liu, J. Yang, Y.H. Zhang, and R.B. Li, Effect of C and Si contents on microstructure and impact toughness in CGHAZ of offshore engineering steel, *Metall. Res. Technol.*, 119(2022), No. 6, art. No. 615.
[131] Y. Zhang, G.H. Shi, R. Sun, K. Guo, C.L. Zhang, and Q.F. Wang, Effect of Si content on the microstructures and the impact properties in the coarse-grained heat-affected zone (CGHAZ) of typical weathering steel, *Mater. Sci. Eng. A*, 762(2019), art. No. 138082.
[132] X.Q. Pan, J. Yang, Y.H. Zhang, L.Y. Xu, and R.B. Li, Effects of Al addition on austenite grain growth, submicrometre and nanometre particles in heat-affected zone of steel plates with Mg deoxidation, *Ironmaking Steelmaking*, 48(2021), No. 4, p. 417.
[133] X.Q. Pan, J. Yang, Q.D. Zhong, *et al*., Effects of coarse particles, prior austenite grains, and microstructures on impact toughness in heat-affected zone of Mg deoxidation steel plates without or with Al addition, *Ironmaking Steelmaking*, 48(2021), No. 8, p. 962.
[134] D.K. Liu, J. Yang, Y.H. Zhang, and L.Y. Xu, Effect of Mo content on nano-scaled particles, prior austenite grains and impact toughness of CGHAZ in offshore engineering steels, *J. Iron Steel Res. Int.*, 29(2022), No. 5, p. 846.
[135] J. Moon, S. Kim, H. Jeong, J. Lee, and C. Lee, Influence of Nb addition on the particle coarsening and microstructure evolution in a Ti-containing steel weld HAZ, *Mater. Sci. Eng. A*, 454-455(2007), p. 648.
[136] X.Q. Pan, J. Yang, and Y.H. Zhang, Microstructure evolution in heat-affected zone of shipbuilding steel plates with Mg deoxidation containing different Nb contents, *Metall. Mater. Trans. A*, 53(2022), No. 4, p. 1512.
[137] T.T. Li, J. Yang, Y.H. Zhang, Y.L. Chen, and Y.Q. Zhang, Particles, microstructures, and impact toughness of CGHAZ of Ca deoxidation shipbuilding steel plates with different Nb contents, *Steel Res. Int.*, 94(2023), No. 8, art. No. 2300020.
[138] Y.L. Yang, X. Jia, Y.X. Ma, *et al*., Effect of Nb on microstructure and mechanical properties between base metal and high heat input coarse-grain HAZ in a Ti-deoxidized low carbon high strength steel, *J. Mater. Res. Technol.*, 18(2022), p. 2399.
[139] C. Wang, J.J. Hao, J. Kang, G. Yuan, R.D.K. Misra, and G.D. Wang, Tailoring the microstructure of coarse-grained HAZ in steel for large heat input welding: Effect of Ti–Mg–Ce–V inclusion/precipitation particles, *Metall. Mater. Trans. A*, 52(2021), No. 8, p. 3191.
[140] S.Y. Han, S.Y. Shin, C.H. Seo, *et al*., Effects of Mo, Cr, and V additions on tensile and charpy impact properties of API X80 pipeline steels, *Metall. Mater. Trans. A*, 40(2009), No. 8, p. 1851.
[141] Y. Liu, Y.H. Sun, and H.T. Wu, Effects of chromium on the microstructure and hot ductility of Nb-microalloyed steel, *Int. J. Miner. Metall. Mater.*, 28(2021), No. 6, p. 1011.
[142] S.S. Babu and H.K.D.H. Bhadeshia, Transition from bainite to acicular ferrite in reheated Fe–Cr–C weld deposits, *Mater. Sci. Technol.*, 6(1990), No. 10, p. 1005.
[143] J.C.F. Jorge, L.F.G. Souza, and J.M.A. Rebello, The effect of chromium on the microstructure/toughness relationship of C–Mn weld metal deposits, *Mater. Charact.*, 47(2001), No. 3-4, p. 195.
[144] G. Huang, X.L. Wan, and K.M. Wu, Effect of Cr content on microstructure and impact toughness in the simulated coarse-grained heat-affected zone of high-strength low-alloy steels, *Steel Res. Int.*, 87(2016), No. 11, p. 1426.
[145] X.Y. Wu, P.C. Xiao, S.J. Wu, *et al*., Effect of molybdenum on the impact toughness of heat-affected zone in high-strength low-alloy steel, *Materials*, 14(2021), No. 6, art. No. 1430.
[146] G.M. Hua, C.S. Li, X.N. Cheng, *et al*., First-principles study on influence of molybdenum on acicular ferrite formation on TiC particles in microallyed steels, *Solid State Commun.*, 269(2018), p. 102.
[147] X.Q. Pan, J. Yang, and Y.H. Zhang, Effect of B segregation at prior austenite grain boundaries on microstructures and toughness in the heat-affected zone of Mg-deoxidized shipbuilding steel plates, *Steel Res. Int.*, 93(2022), No. 8, art. No. 2200102.
[148] Y. Chen, D.T. Zhang, Y.C. Liu, H.J. Li, and D.K. Xu, Effect of dissolution and precipitation of Nb on the formation of acicular ferrite/bainite ferrite in low-carbon HSLA steels, *Mater. Charact.*, 84(2013), p. 232.
[149] D.K. Liu, J. Yang, and Y.H. Zhang, Effect of boron content on microstructure and impact toughness in CGHAZ of shipbuilding steel plates with Ca deoxidation, *Steel Res. Int.*, 94(2023), No. 3, art. No. 2200278.